

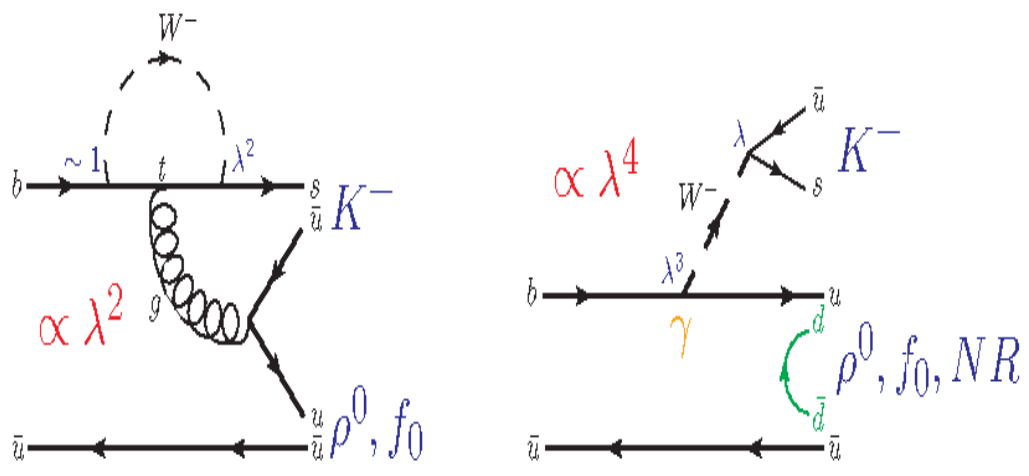


Charmless $B^\pm \rightarrow h^\pm h^+ h^-$ decays at LHCb

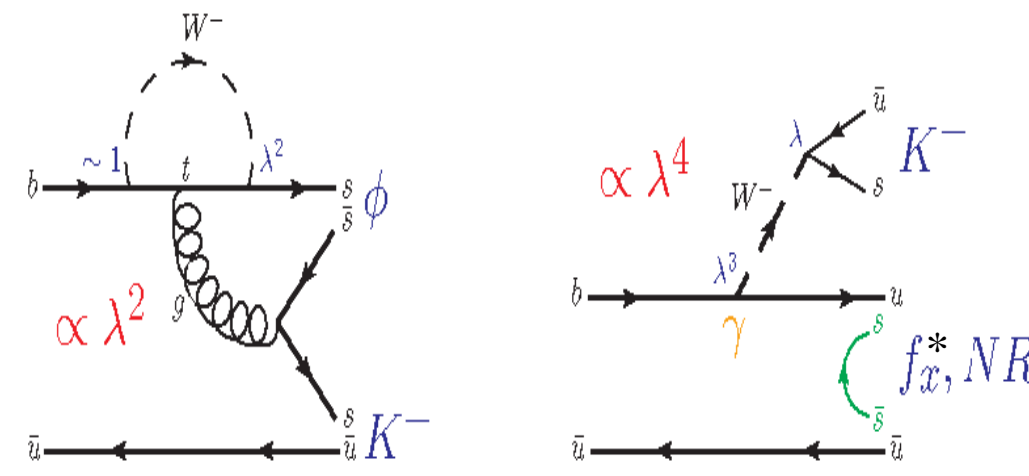
Alvaro Gomes on behalf of LHCb collaboration
(Universidade Federal do Triângulo Mineiro)

- Theory Overview
 - The $B^\pm \rightarrow h^\pm h^+ h^-$ charmless decays.
 - Dalitz plot.
- Evidence of direct CP violation in $B^\pm \rightarrow K^\pm \pi^+ \pi^-$ and $B^\pm \rightarrow K^\pm K^+ K^-$ decays.
[LHCb-CONF-2012-018](#) preliminary $\mathcal{L} = 1.0 \text{ fb}^{-1}$
- Evidence of direct CP violation in $B^\pm \rightarrow \pi^\pm K^+ K^-$ and $B^\pm \rightarrow \pi^\pm \pi^+ \pi^-$ decays.
[LHCb-CONF-2012-028](#) preliminary $\mathcal{L} = 1.0 \text{ fb}^{-1}$
- Measurements of the branching fraction of $B^+ \rightarrow p \bar{p} K^+$ decays.
[LHCb-PAPER-2012-047](#) preliminary $\mathcal{L} = 1.0 \text{ fb}^{-1}$
- Conclusions

$B^\pm \rightarrow K^\pm \pi^+ \pi^-$ BR $\propto 10^{-5}$



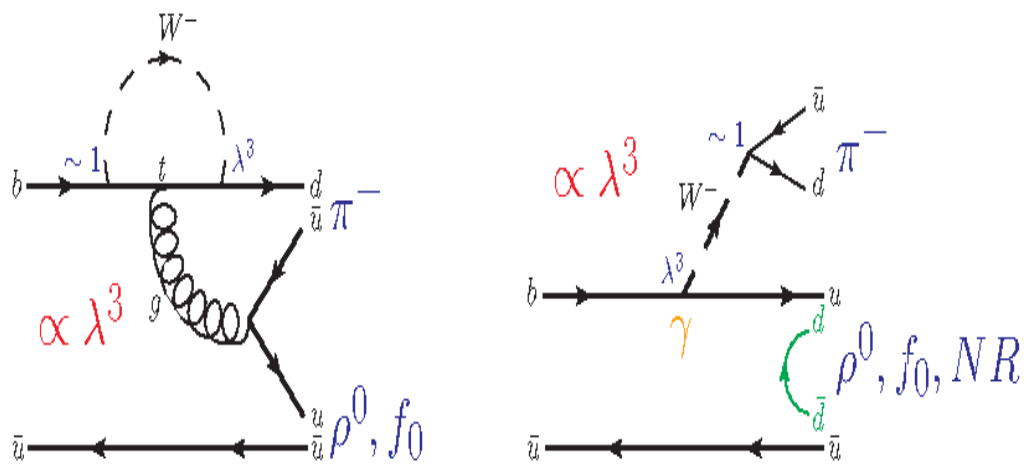
$B^\pm \rightarrow K^\pm K^+ K^-$ BR $\propto 10^{-5}$



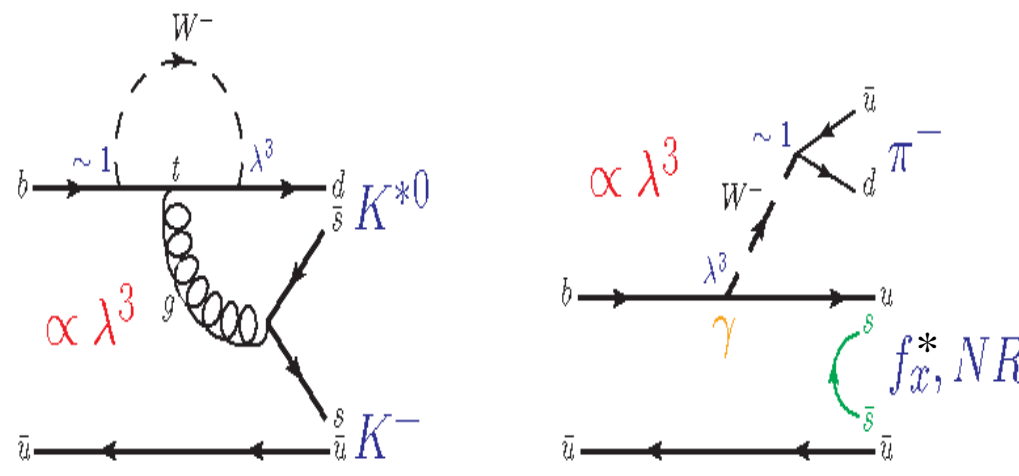
- Access to $t \rightarrow s$ (P) and the CKM phase $b \rightarrow u$ (T) transitions.
 - γ at tree level.
- CP violation (CPV) expected from interference between tree ($\propto \lambda^4$) and penguin ($\propto \lambda^2$) diagrams in both channels. **Type I**
- For $K\pi\pi$:
 - CP violation expected also from ρ^0, f_0 and K^* interferences in the phase space. **Type II**
- For KKK :
 - ϕ resonance only from penguin contribution.
 - CPV expected only from interference between ϕ and f_x (or no-resonant). **Type II**
- Note that **Type I** and **Type II** are two different sources of CPV.

* f_x holds for any resonance with the K^+K^- final state.

$B^\pm \rightarrow \pi^\pm \pi^+ \pi^-$ BR $\propto 10^{-5}$



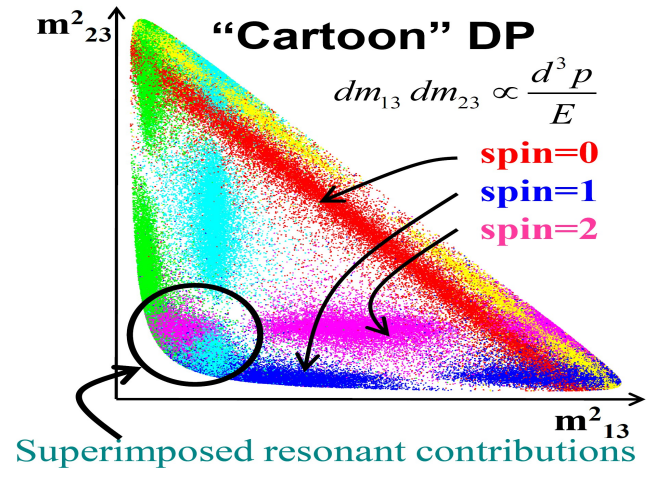
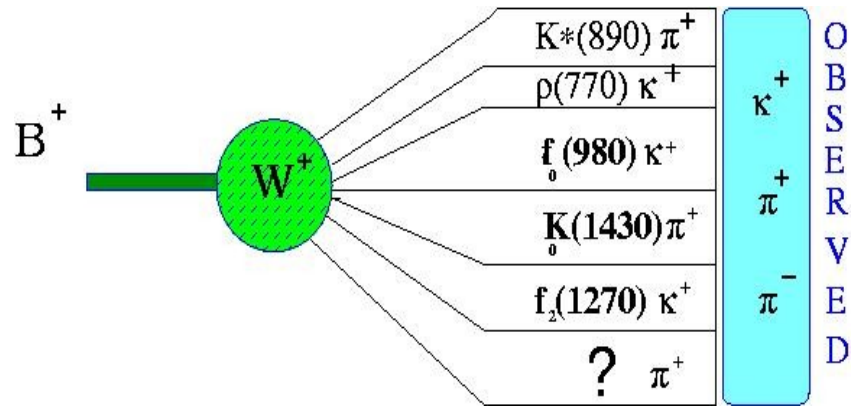
$B^\pm \rightarrow \pi^\pm K^+ K^-$ BR $\propto 10^{-6}$



- Access to $t \rightarrow d$ (P) and the CKM phase $b \rightarrow u$ (T) transitions.
 - γ at tree level.
- CPV expected from interference between tree ($\propto \lambda^3$) and penguin ($\propto \lambda^3$) diagrams in both channels. **Type I**
- For $\pi\pi\pi$:
 - CP violation expected also from ρ^0 and f_0 interferences in the phase space. **Type II**
- For πKK :
 - ϕ resonance not expected for this mode (for current LHCb statistics).
 - CPV expected only from interference between K^* and f_x (or no-resonant). **Type II**
- Note that **Type I** and **Type II** are two different sources of CPV.

* f_x holds for any resonance with the K^+K^- final state.

- CPV in Dalitz plot (DP) is commonly studied through an amplitude analysis using the isobar model:

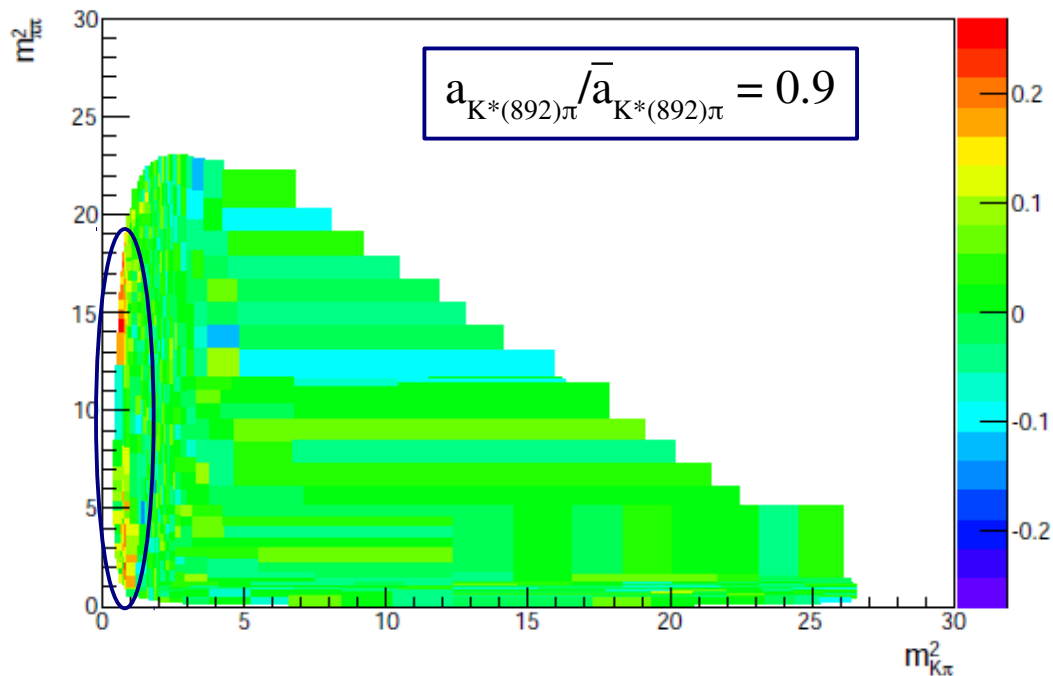


$$\mathcal{A}(B \rightarrow f) = \sum a_r e^{i(\varphi)} \mathcal{M}_r + \sum a_r e^{i(\varphi + \gamma)} \mathcal{M}_r + a_{nr} e^{i\delta} \mathcal{M}_{nr}$$

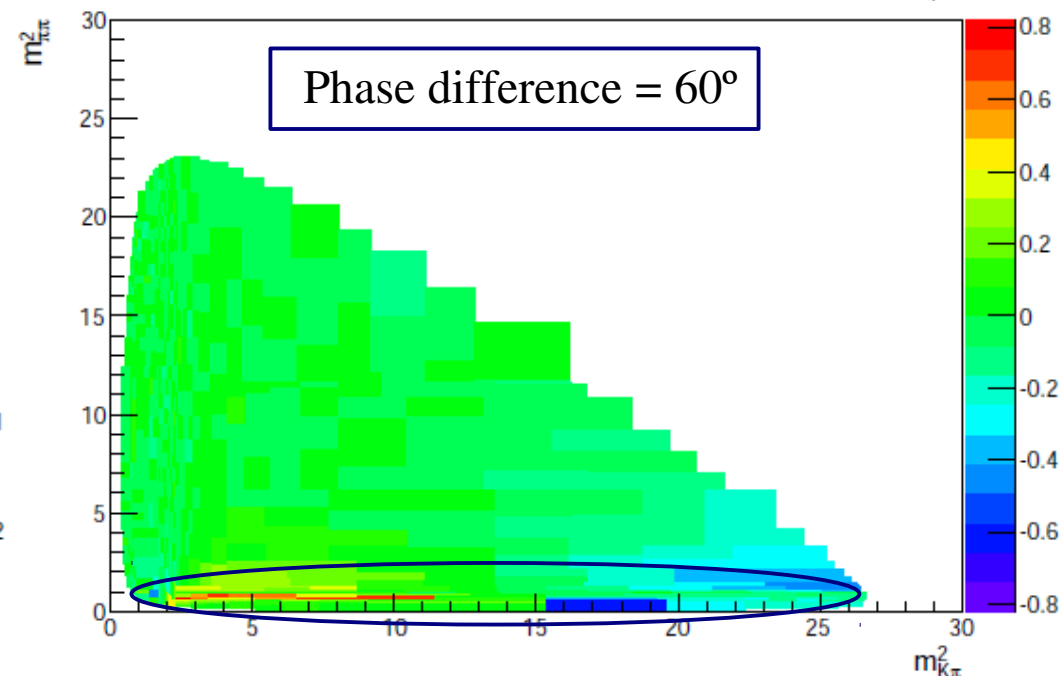
- Each resonance is included in a coherent sum for the total decay.
- Resonance interferences (parallel or crossing) \rightarrow probe for CPV.
- CPV comes from differences in the amplitudes and phases for \mathcal{A} and $\overline{\mathcal{A}}$.
 - Strong phase φ don't change sign under $\mathcal{A} \rightarrow \overline{\mathcal{A}}$.
 - Weak phase γ changes the under $\mathcal{A} \rightarrow \overline{\mathcal{A}}$.
- Some results in these modes:
 - Belle and BaBar: Evidence of CPV in $B^\pm \rightarrow \rho K^\pm$ ($K\pi\pi$ final state). Belle: PRL **96**, (2006) 251803 BaBar: PR **D78**, (2008) 012004
 - BaBar: Evidence of CPV in $B^\pm \rightarrow \phi K^\pm$ (KKK final state). BaBar: PR **D85**, (2012) 112010

- Amplitude analysis has a characteristic feature:
 - Difference in the amplitude for a resonance implies a difference in the total number of events for that resonance.
 - Difference in weak phase for a resonance implies a change in the shape of the resonance band in the phase space.
- Both effects must be seen where the resonance exists.

Fast MC with amplitude difference in $K^*\pi$



Fast MC with phase difference in ρK_s



- Selection explores the decay topology:
 - Tracks with high momentum and transverse momentum.
 - Tracks with large impact parameters with respect to the interaction point.
 - B candidate with large flight distance, momentum and impact parameter with respect to interaction point.
- Particle ID used to separate kaons from pions and to veto muons.
- Different samples based on different trigger decisions used for the measurement.
- Observable:

$$A_{\text{cp}} = \frac{\Gamma(B^{-} \rightarrow f) - \Gamma(B^{+} \rightarrow f)}{\Gamma(B^{-} \rightarrow f) + \Gamma(B^{+} \rightarrow f)}$$

- The raw asymmetry can be interpreted as:

$$A_{\text{cp}}^{\text{RAW}}(\text{K}^{\pm}\text{h}^+\text{h}^-) = A_{\text{cp}}(\text{K}^{\pm}\text{h}^+\text{h}^-) + A_{\text{p}}(\text{B}^{\pm}) + A_{\text{I}}(\text{K}^{\pm})$$

- Where:
 - A_{cp} is the physical CPV.
 - A_{p} is the B^+/B^- production asymmetry.
 - $A_{\text{I}}(\text{K}^{\pm})$ is the instrumental asymmetry that holds for kaon detection and reconstruction.
- The $\text{B}^{\pm} \rightarrow \text{J}/\psi\text{K}^{\pm}$ mode is used to extract the A_{I} and A_{p} asymmetries.
 - Same decay topology as $\text{B}^{\pm} \rightarrow \text{h}^{\pm}\text{h}^+\text{h}^-$ decays and same selection applied.
 - A_{p} is independent of the final state.
 - No CPV expected: $A_{\text{CP}} = 0.001 \pm 0.007$. **PDG**

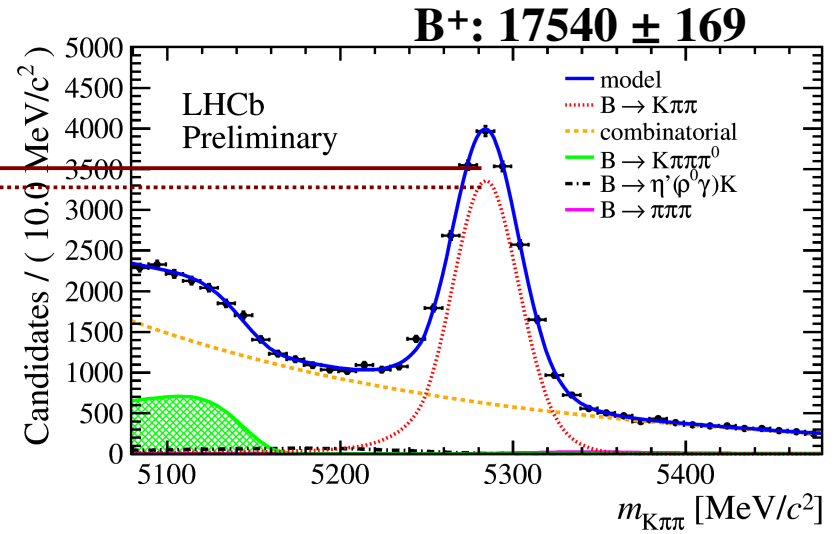
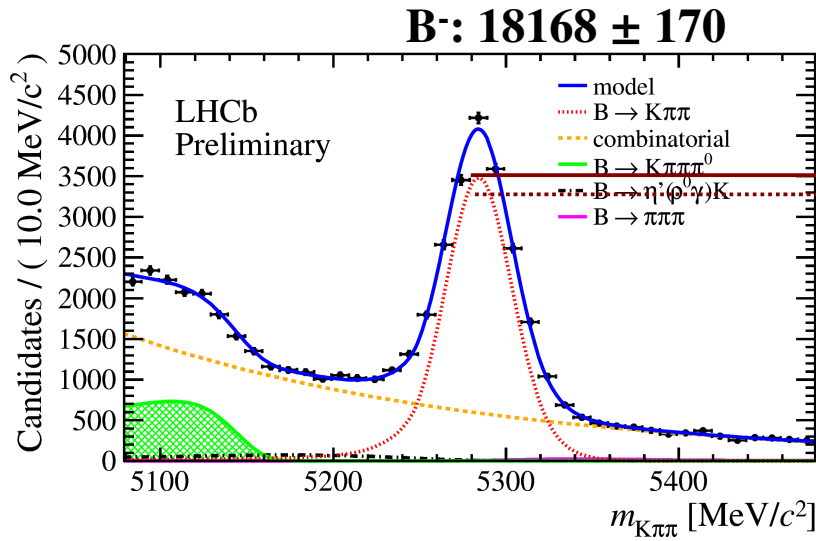
$$A_{\text{cp}}^{\text{raw}}(\text{J}/\psi\text{K}) = -0.014 \pm 0.004$$

- Hence:

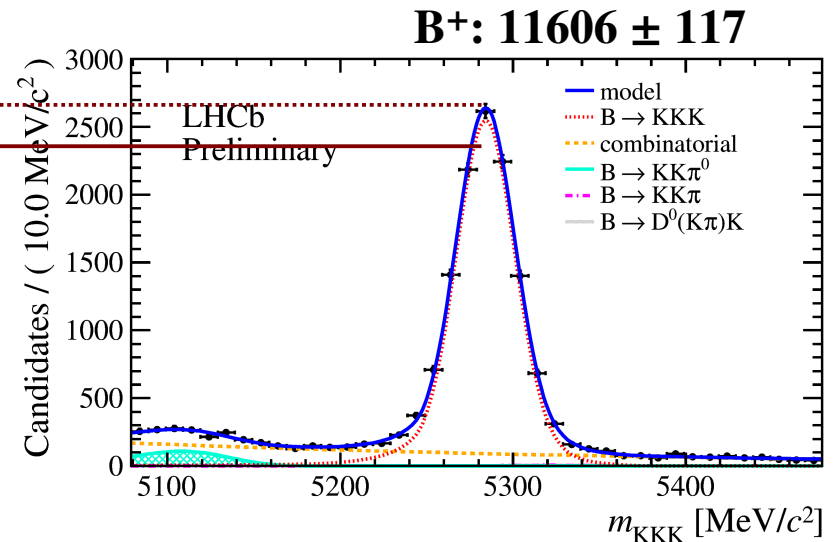
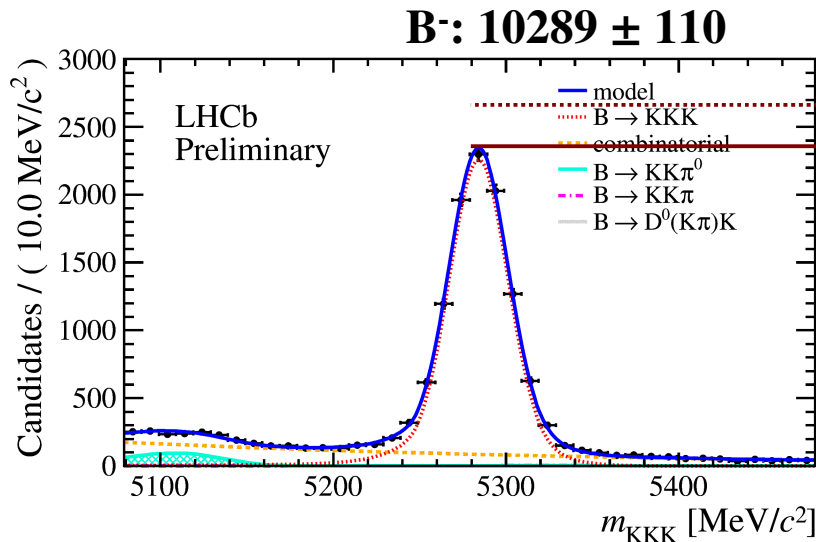
$$A_{\text{p}}(\text{B}^{\pm}) + A_{\text{I}} = A_{\text{cp}}^{\text{RAW}}(\text{J}/\psi\text{K}^{\pm}) - A_{\text{cp}}(\text{J}/\psi\text{K}^{\pm})$$

$$A_{\text{cp}}(\text{K}^{\pm}\text{h}^+\text{h}^-) = A_{\text{cp}}^{\text{RAW}}(\text{K}^{\pm}\text{h}^+\text{h}^-) - A_{\text{cp}}^{\text{RAW}}(\text{J}/\psi\text{K}^{\pm}) + A_{\text{cp}}(\text{J}/\psi\text{K}^{\pm})$$

$B^\pm \rightarrow K^\pm \pi^+ \pi^-$ and $B^\pm \rightarrow K^\pm K^+ K^-$ raw asymmetries



$$A_{cp}^{\text{raw}}(K\pi\pi) = +0.018 \pm 0.007$$



$$A_{cp}^{\text{raw}}(KKK) = -0.060 \pm 0.007$$

$B^\pm \rightarrow K^\pm \pi^+ \pi^-$ and $B^\pm \rightarrow K^\pm K^+ K^-$ systematics and results

- The main sources of systematic uncertainties are:
 - Subtraction method: kinematic variables of the kaon from control channel were weighted to match the same distribution from the signal kaon.
 - Trigger correction: the measurement was performed using samples from different trigger decision.
- Final result:

$$A_{\text{cp}}(B^\pm \rightarrow K\pi\pi) = +0.034 \pm 0.009(\text{stat}) \pm 0.004(\text{syst}) \pm 0.007(J/\psi K)$$

2.8σ

$$A_{\text{cp}}(B^\pm \rightarrow KKK) = -0.046 \pm 0.009(\text{stat}) \pm 0.005(\text{syst}) \pm 0.007(J/\psi K)$$

3.7σ

- Previous measurements:

$$A_{\text{cp}}(B^\pm \rightarrow K\pi\pi) = +0.038 \pm 0.022$$

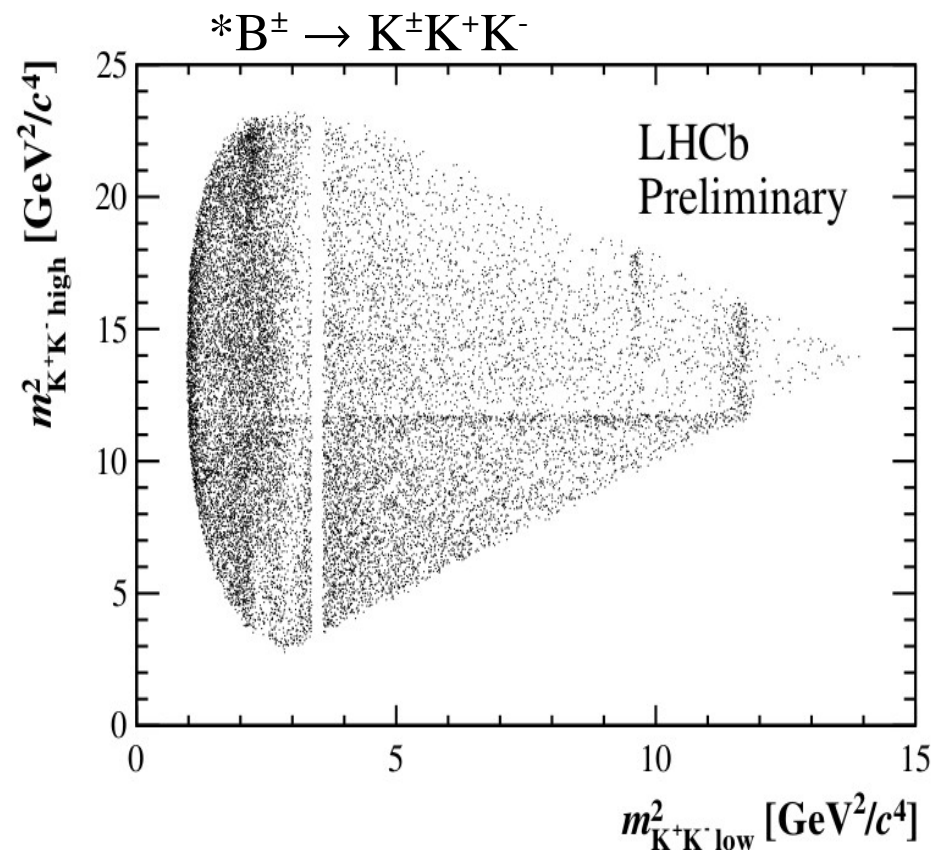
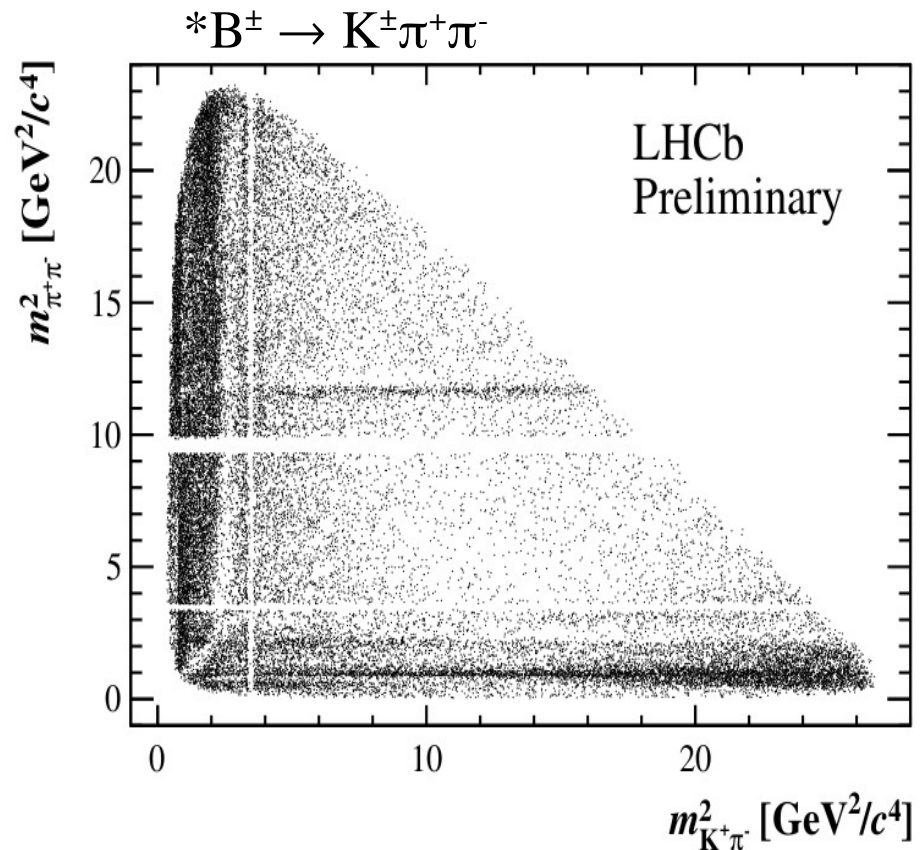
$$A_{\text{cp}}(B^\pm \rightarrow KKK) = -0.017 \pm 0.030$$

PDG

First evidence of global CPV
in charmless
three-body B decays.



$B^\pm \rightarrow K^\pm \pi^+ \pi^-$ and $B^\pm \rightarrow K^\pm K^+ K^-$ Dalitz plot

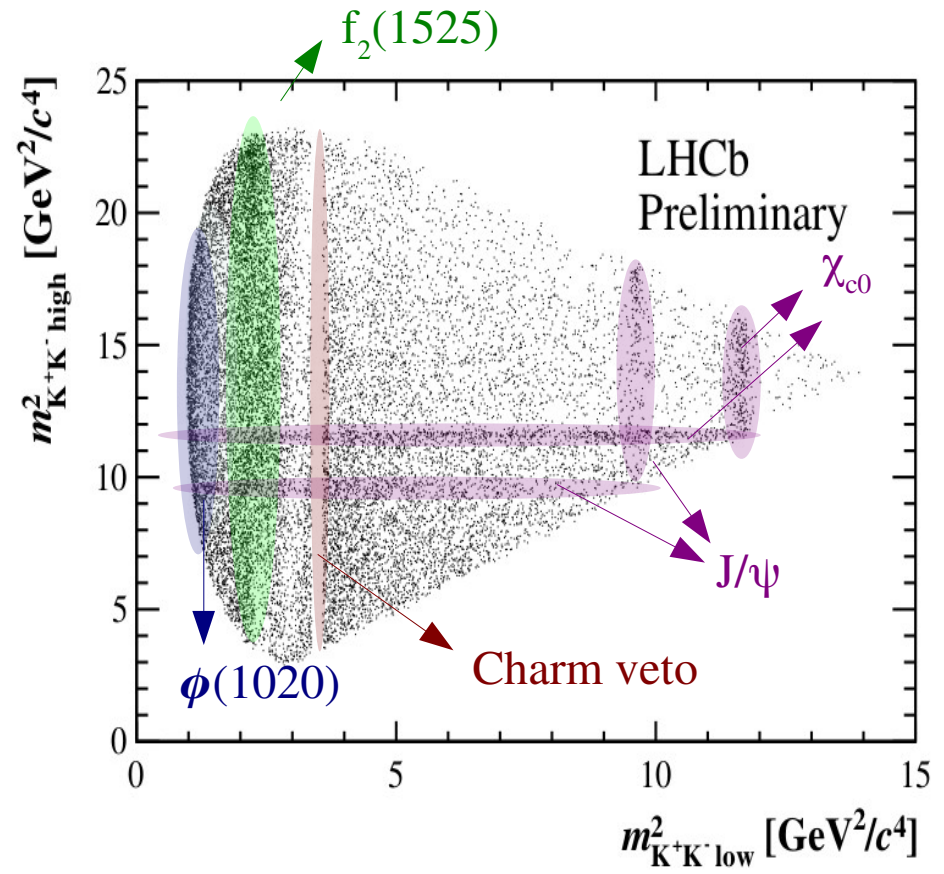
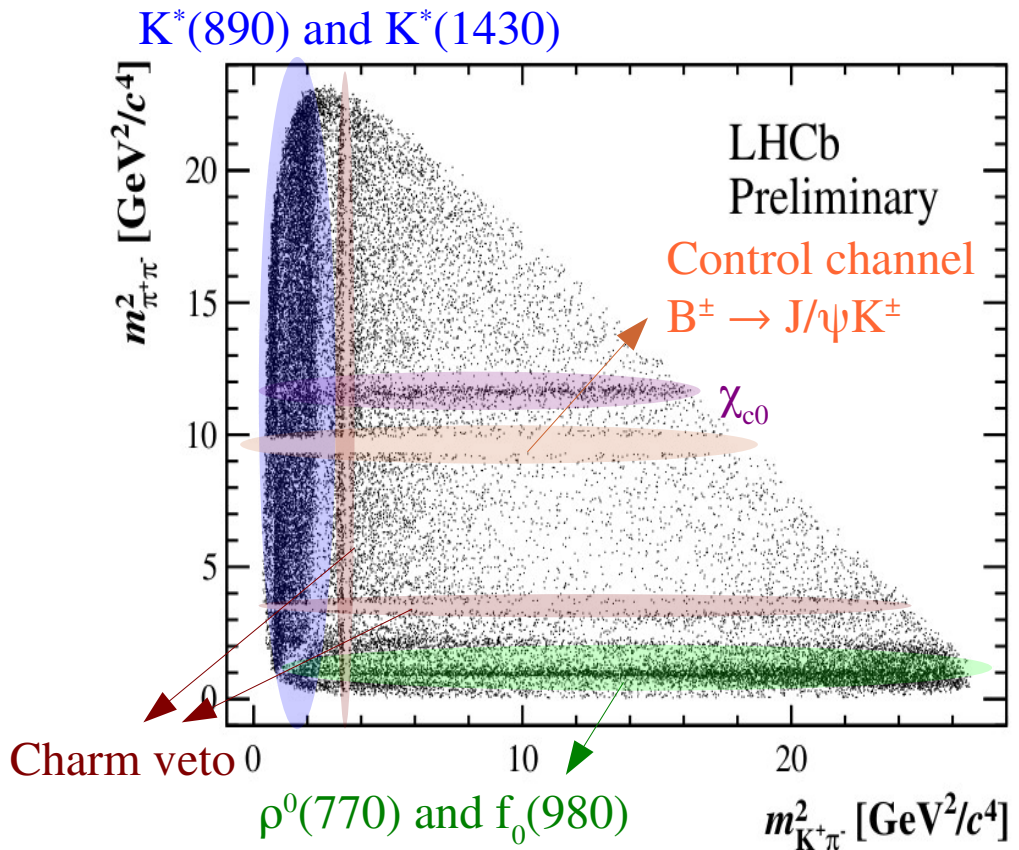


- Phase space without B mass constraint.
- Phase space not background subtracted.
- D^0 contribution removed.
- J/ψ contribution removed from $K\pi\pi$ sample since it is the control channel.
- Acceptance efficiency is flat over the Dalitz plot

$$m^2_{K^\pm K^\mp \text{ Low}} < m^2_{K^\pm K^\mp \text{ High}}$$

* $\pm 40 \text{ MeV } m_B$ mass window

$B^\pm \rightarrow K^\pm \pi^+ \pi^-$ and $B^\pm \rightarrow K^\pm K^+ K^-$ Dalitz plot



$$m^2_{K^\pm K^\mp Low} < m^2_{K^\pm K^\mp High}$$

- Phase space without B mass constraint.
- Phase space not background subtracted.
- D^0 contribution removed.
- J/ψ contribution removed from $K\pi\pi$ sample since it is the control channel.
- Acceptance efficiency is flat over the Dalitz plot

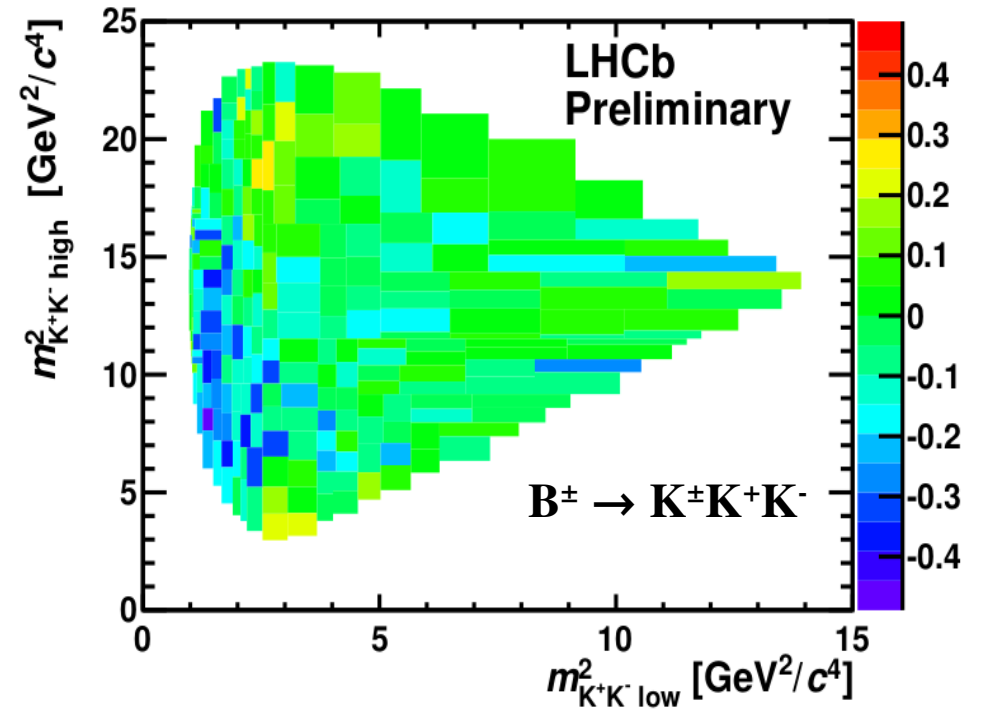
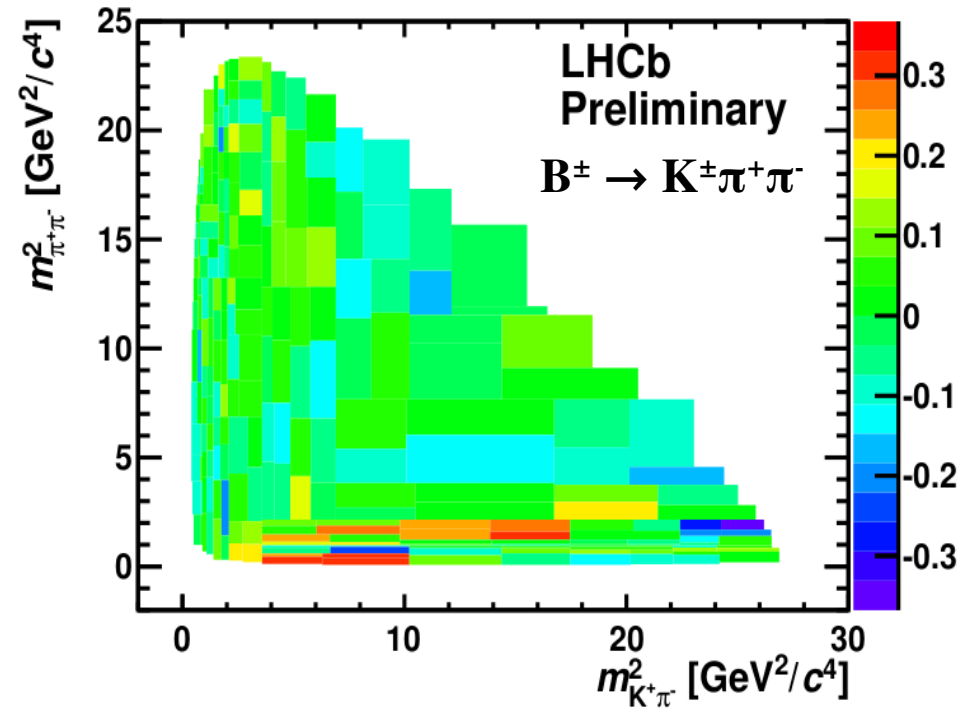


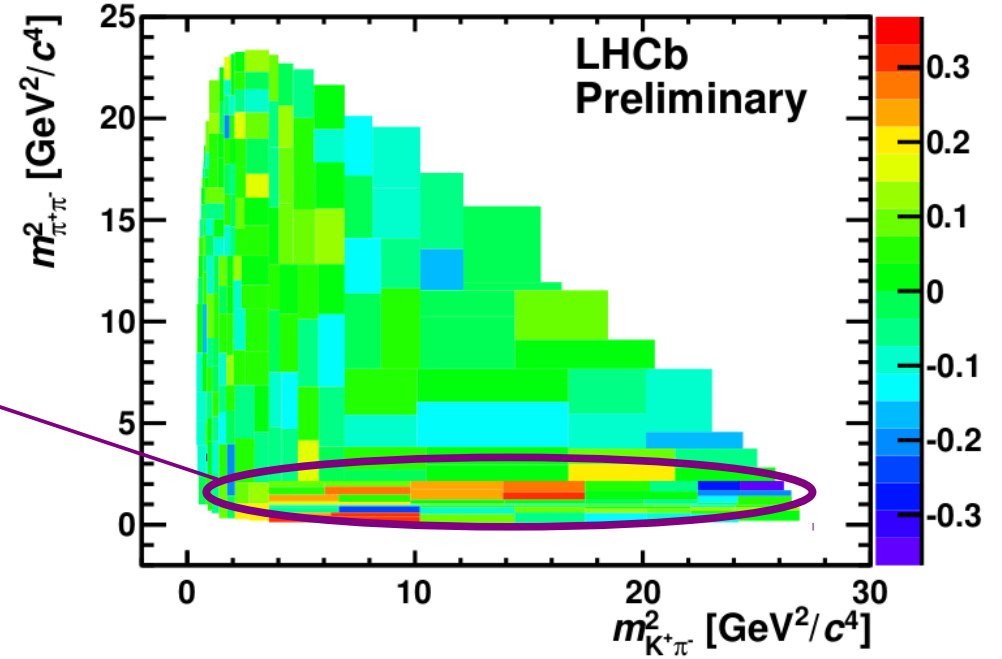
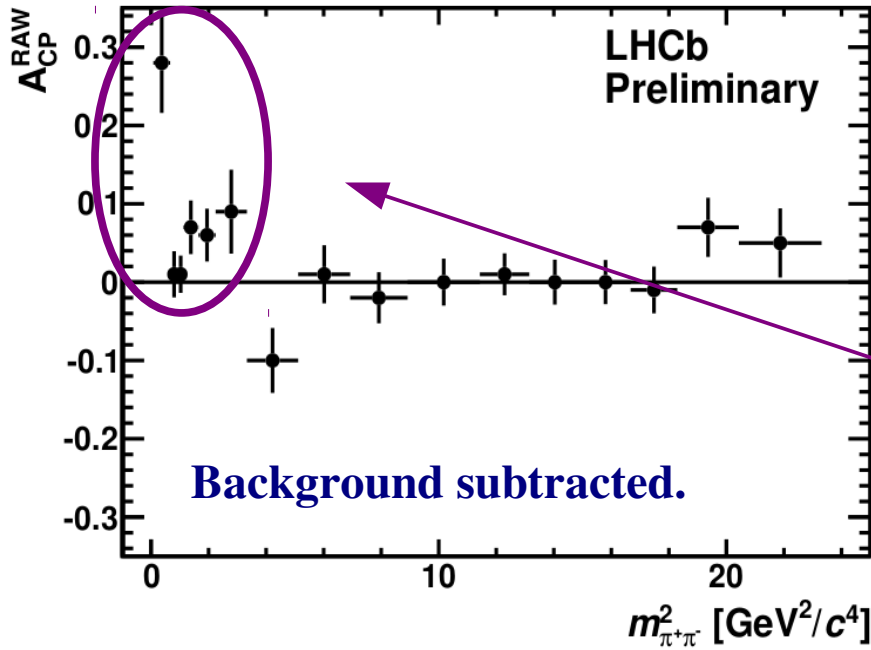
$B^\pm \rightarrow K^\pm \pi^+ \pi^-$ and $B^\pm \rightarrow K^\pm K^+ K^-$ Dalitz plot

- Different approaches for Dalitz plots:
 - Adaptive binning applied to define bins with equal number of entries for the total sample.
- Asymmetry per bin (including background):

$$A_{cp}^N(s, b) = \frac{(s + b)^- - (s + b)^+}{(s + b)^- + (s + b)^+}$$

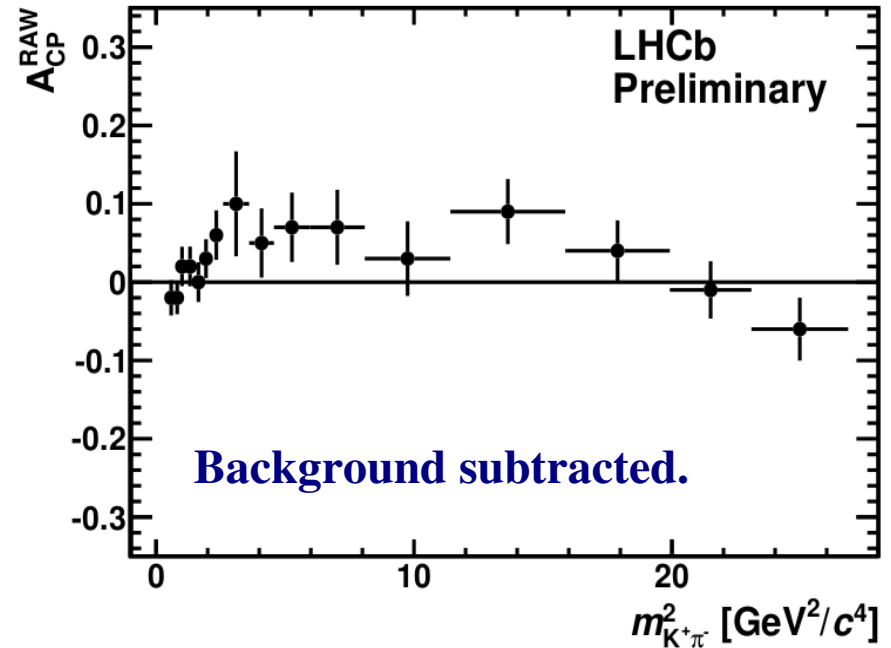
- The A_{cp}^n for each bin was computed:

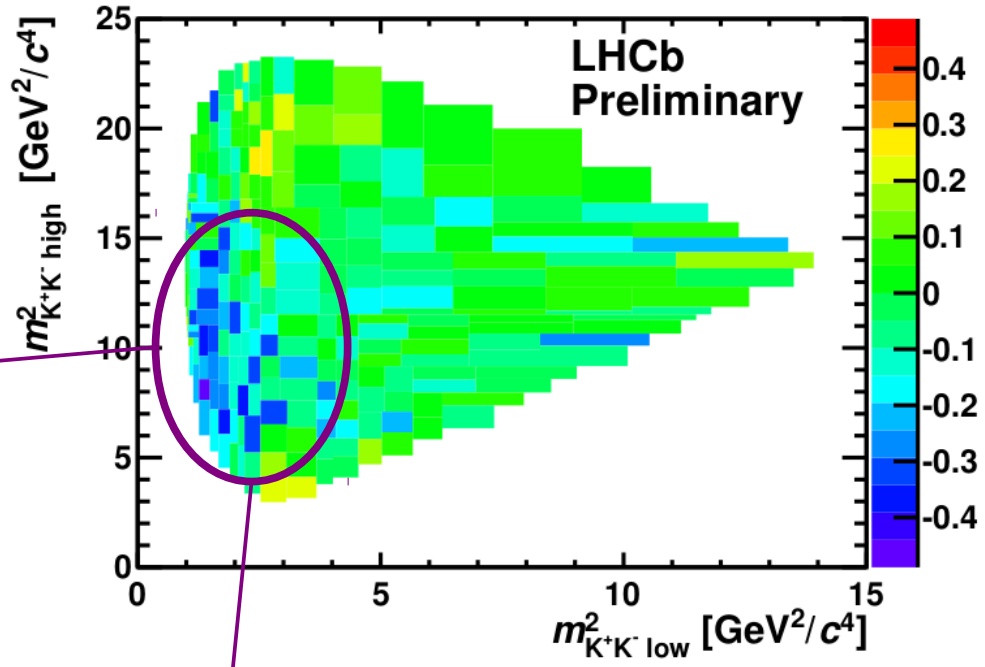
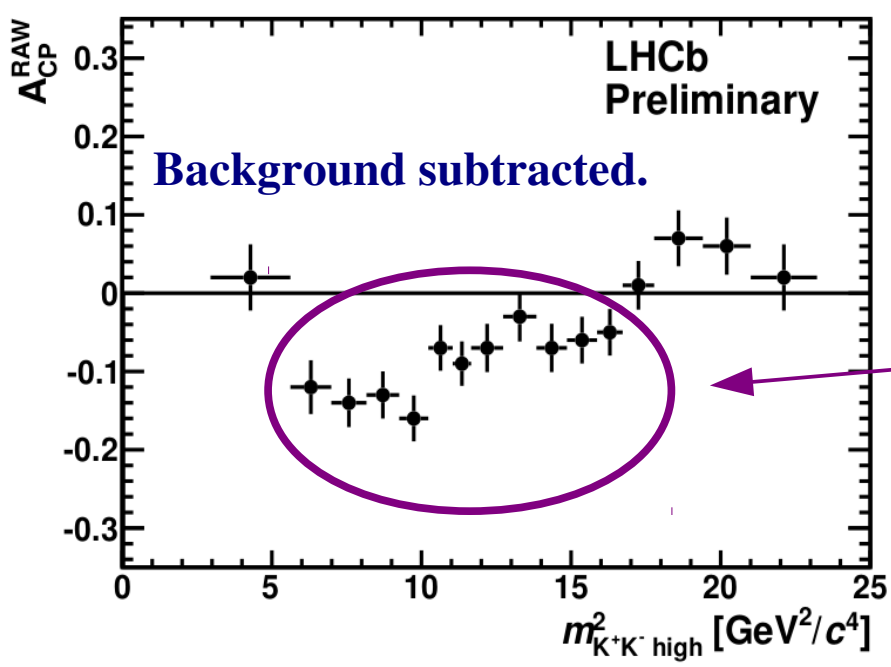




- Agrees with B factories results.
- No signature of CPV in the $K\pi$ invariant mass

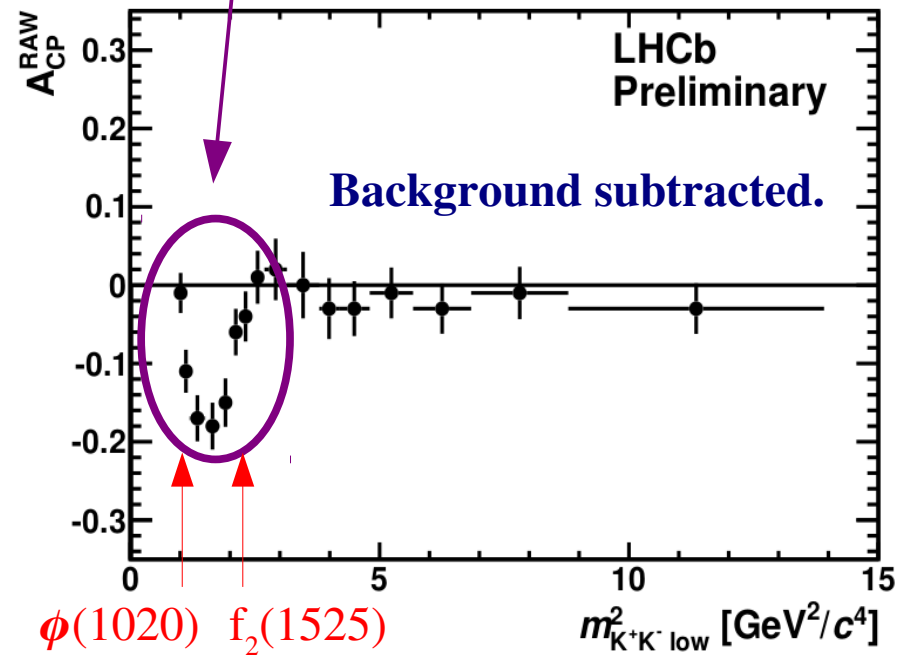
Large positive CPV at low $m^2_{\pi^+\pi^-}$





- No similar report from B factories.

Very large CPV at low $m^2_{K^+K^- \text{ low}}$ not clearly associated to a resonance





$B^\pm \rightarrow \pi^\pm \pi^+ \pi^-$ and $B^\pm \rightarrow \pi^\pm K^+ K^-$

LHCb-CONF-2012-028

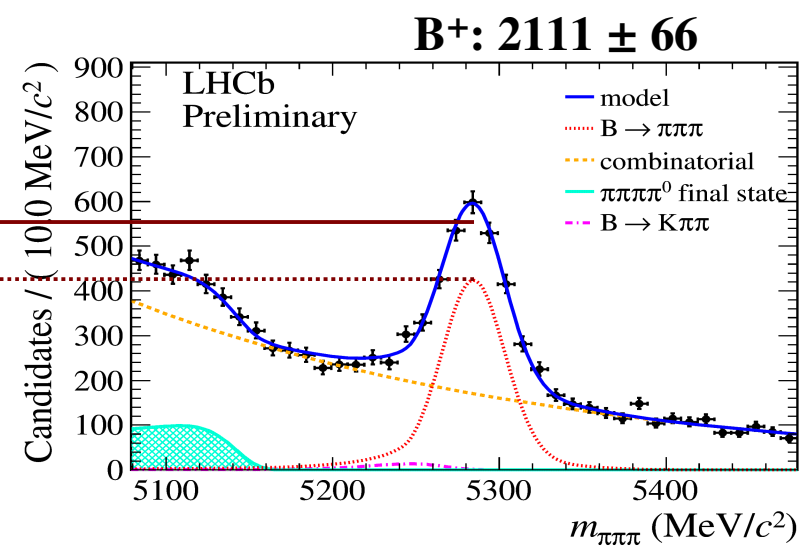
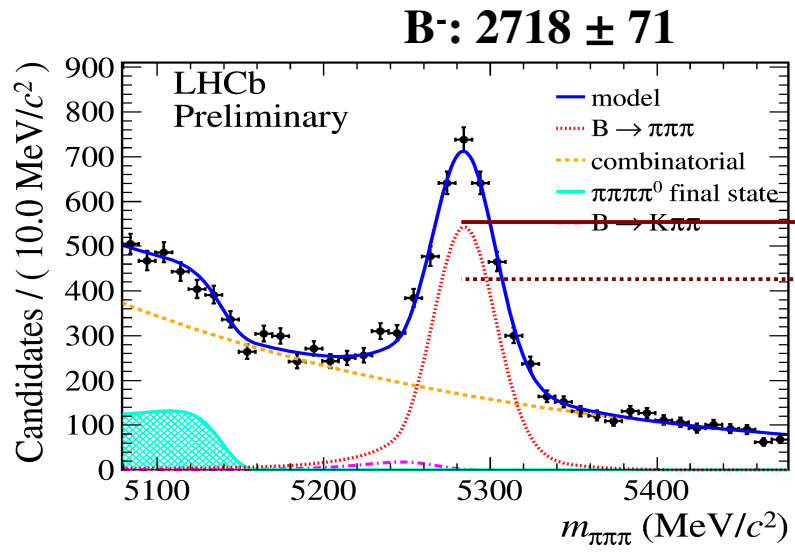
- Same selection applied on $B^\pm \rightarrow K^\pm \pi^+ \pi^-$ and $B^\pm \rightarrow K^\pm K^+ K^-$ analysis.
- Particle ID used to separate kaons from pions and to veto muons.
- Different samples based on different trigger decisions used for the measurement.
- Similar statistics
 - Large background.
- Instrumental and productions asymmetries:
 - Even number of kaons.
 - Instrumental asymmetry for pions extracted from a large D^* sample.
 - B^\pm production asymmetry extracted using previous analysis results.

- The raw asymmetry can be interpreted as:

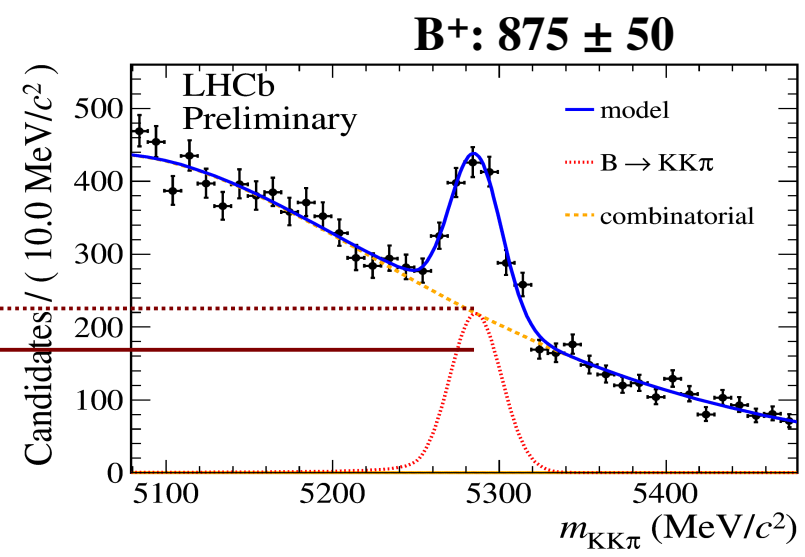
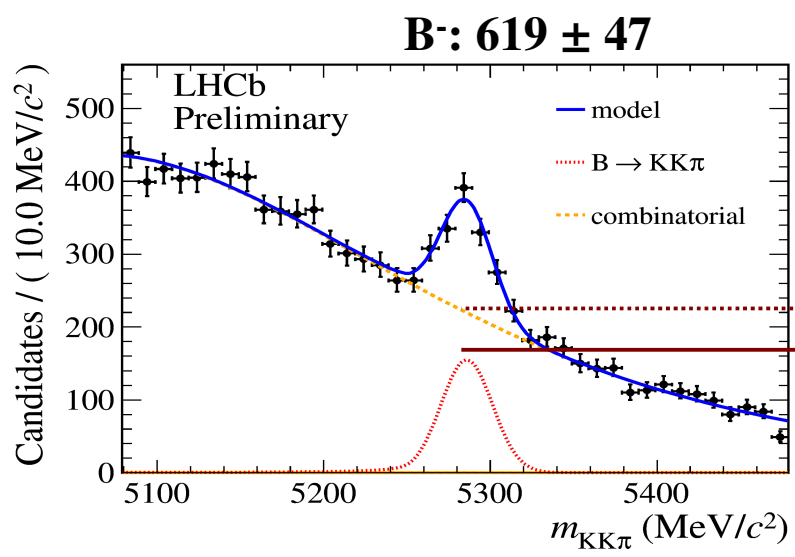
$$A_{\text{cp}}^{\text{RAW}}(\pi^{\pm}h^{+}h^{-}) = A_{\text{cp}}(\pi^{\pm}h^{+}h^{-}) + A_{\text{p}} + A_{\text{I}}$$

- Where:
 - A_{cp} is the physical CPV.
 - A_{p} is the B^{+}/B^{-} production asymmetry.
 - A_{I} is the instrumental asymmetry that holds for detection and reconstruction.
 - $A_{\text{cp}}^{\text{RAW}}$ is the raw asymmetry and it was corrected by the acceptance in the Dalitz plot.
- Base measurements:
 - A_{p} extracted from $B^{\pm} \rightarrow J/\psi K^{\pm}$ control channel. [LHCb-CONF-2012-018](#)
 - Large sample of $D^0 \rightarrow K^{\pm}\pi^{\mp}$ and $D^0 \rightarrow K^{+}K^{-}$ used to measure the $A_{\text{I}}(K^{\pm})$.
[LHCb: PRL 108, \(2012\) 201601.](#)
 - $A_{\text{I}}(\pi^{\pm})$ for pions extracted from a large $D^{*\pm}$ sample. [LHCb: PL B713, \(2012\) 186.](#)

$B^\pm \rightarrow \pi^\pm \pi^+ \pi^-$ and $B^\pm \rightarrow \pi^\pm K^+ K^-$ raw asymmetry



$$A_{cp}^{\text{raw}}(\pi\pi\pi) = +0.125 \pm 0.020$$



$$A_{cp}^{\text{raw}}(\pi KK) = -0.171 \pm 0.046$$

$B^\pm \rightarrow \pi^\pm \pi^+ \pi^-$ and $B^\pm \rightarrow \pi^\pm K^+ K^-$ systematics and results

- The main sources of systematic uncertainties are:
 - Acceptance efficiency: the acceptance over the Dalitz plot was corrected for the B^+ and B^- detection and reconstruction efficiencies.
 - Kaon kinematics: the $B^\pm \rightarrow J/\psi K^\pm$ raw asymmetry in bins of kaon momentum is weighted by the ratio of K^- and K^+ efficiencies from $D^0 \rightarrow K^+ K^-$ sample.
- Final result:

$$A_{cp}(B^\pm \rightarrow \pi\pi\pi) = +0.120 \pm 0.020(\text{stat}) \pm 0.019(\text{syst}) \pm 0.007(J/\psi K)$$

$$A_{cp}(B^\pm \rightarrow \pi K K) = -0.153 \pm 0.046(\text{stat}) \pm 0.019(\text{syst}) \pm 0.007(J/\psi K)$$

4.2 σ

3.0 σ

- Previous measurements:

$$A_{cp}(B^\pm \rightarrow \pi\pi\pi) = +0.032 \pm 0.044(\text{stat}) \begin{matrix} +0.040 \\ -0.037 \end{matrix}(\text{syst})$$

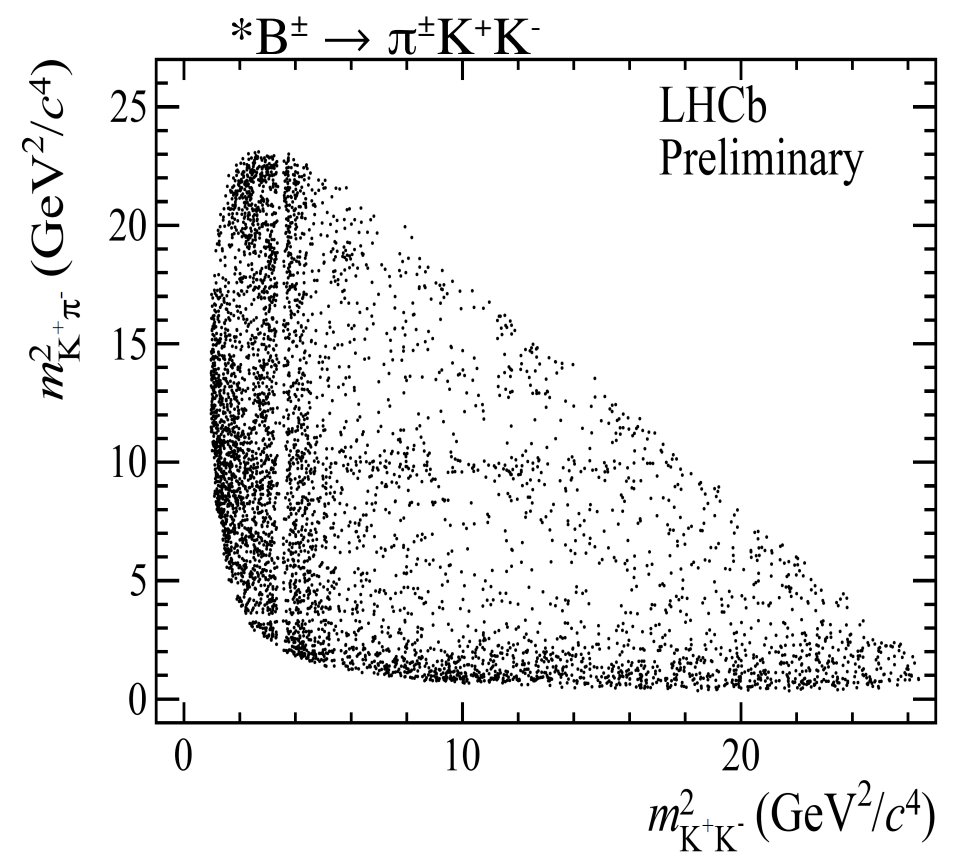
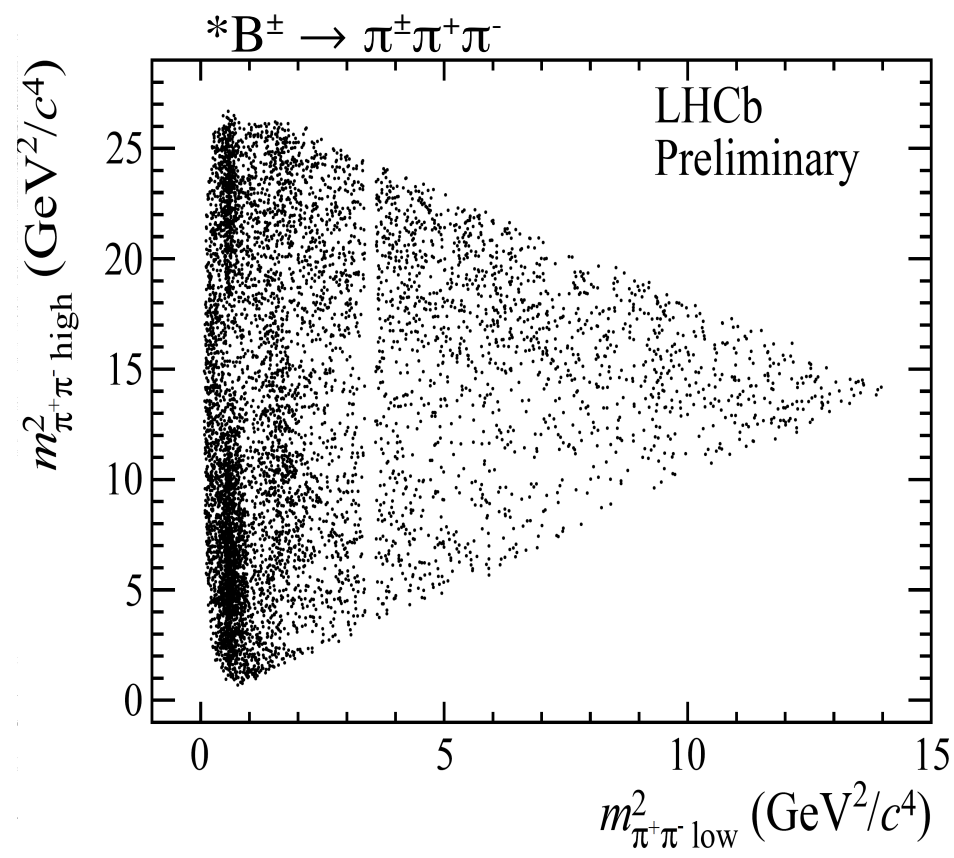
$$A_{cp}(B^\pm \rightarrow \pi K K) = -0.00 \pm 0.10(\text{stat}) \pm 0.03(\text{syst})$$

PDG

First evidence of global CPV
in charmless
three-body B decays.



$B^\pm \rightarrow \pi^\pm \pi^+ \pi^-$ and $B^\pm \rightarrow \pi^\pm K^+ K^-$ Dalitz plot

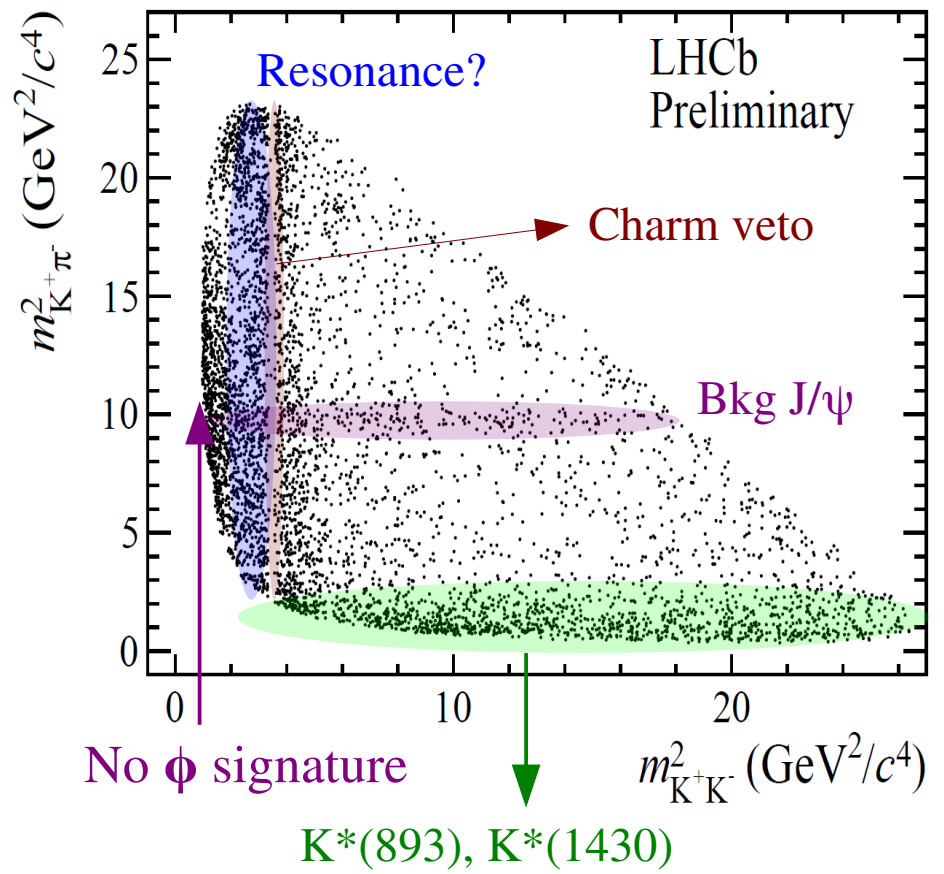
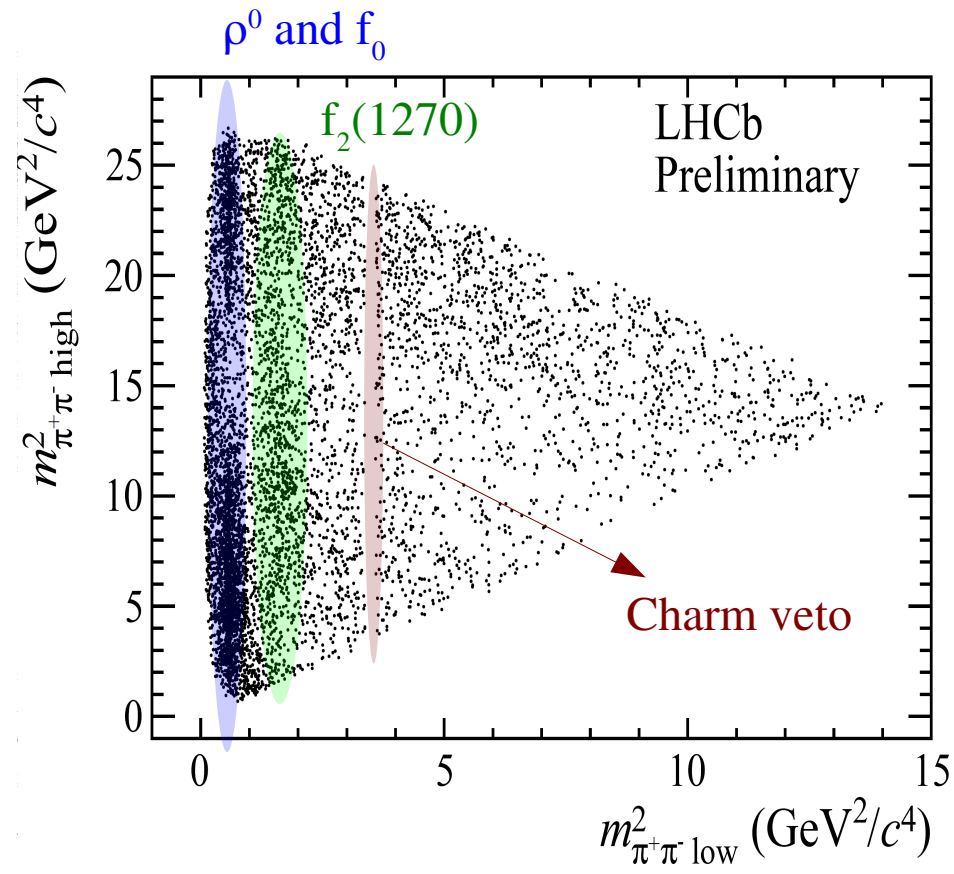


$$m^2_{\pi^+ \pi^- \text{ low}} < m^2_{\pi^+ \pi^- \text{ high}}$$

- Phase space without B mass constraint.
- Phase space not background subtracted.
- D^0 contribution removed.
- Acceptance efficiency is flat over the Dalitz plot

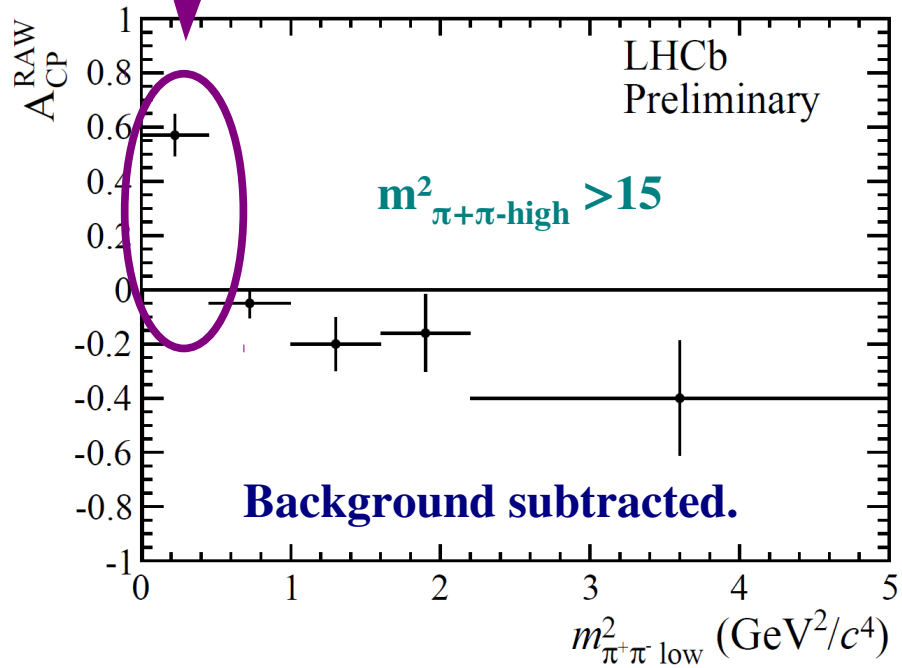
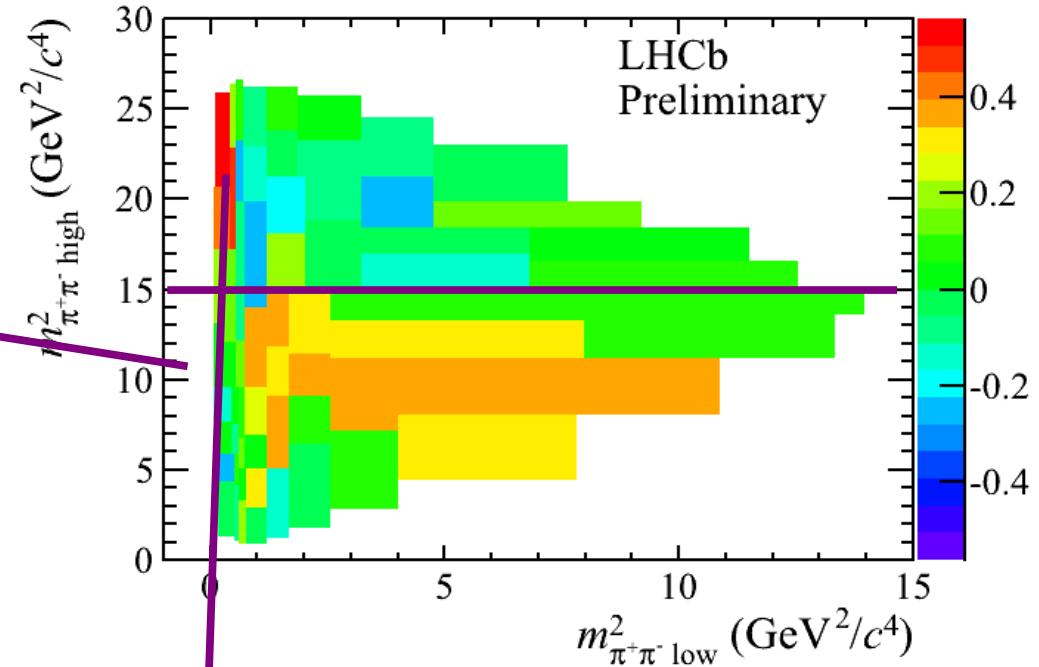
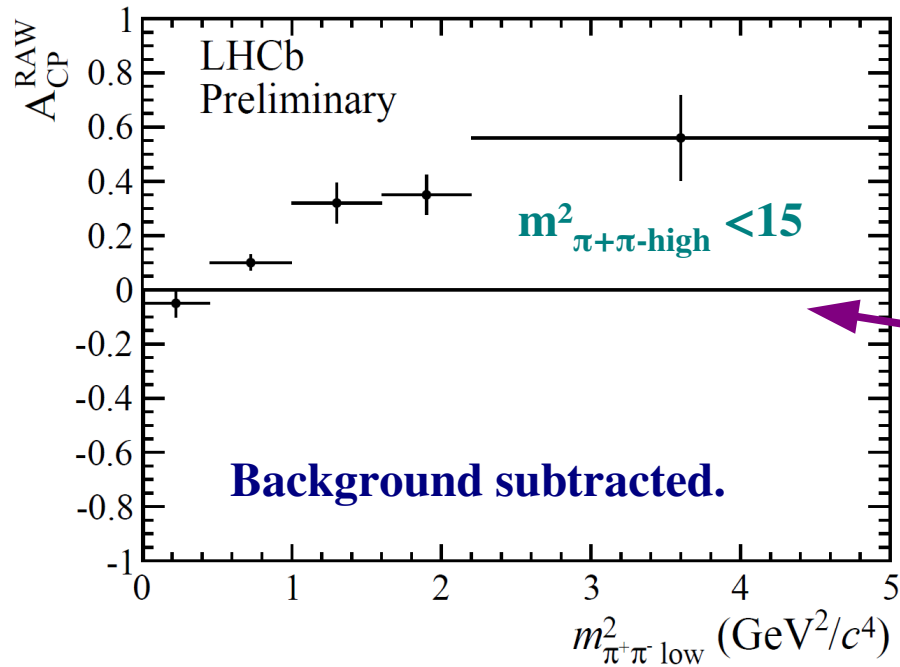
* $\pm 40 \text{ MeV } m_B$ mass window

$B^\pm \rightarrow \pi^\pm \pi^+ \pi^-$ and $B^\pm \rightarrow \pi^\pm K^+ K^-$ Dalitz plot



$$m_{\pi^+ \pi^- \text{ low}}^2 < m_{\pi^+ \pi^- \text{ high}}^2$$

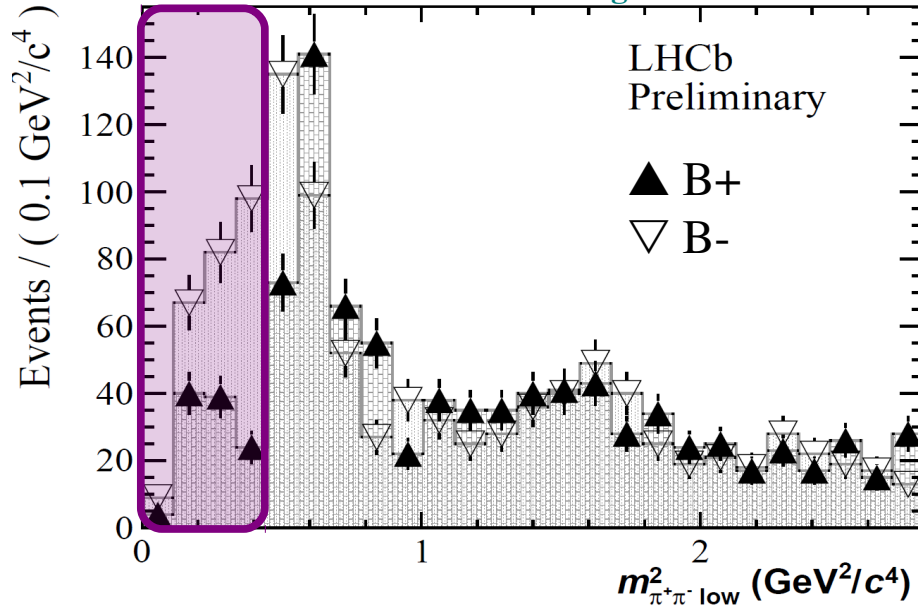
- Phase space without B mass constraint.
- Phase space not background subtracted.
- D^0 contribution removed.
- Acceptance efficiency is flat over the Dalitz plot



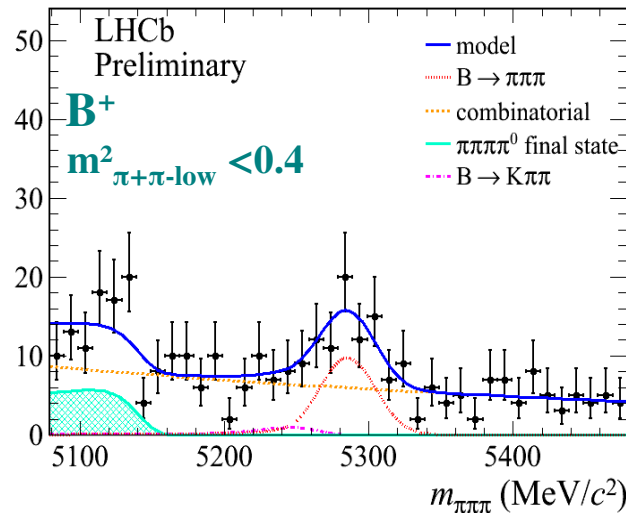
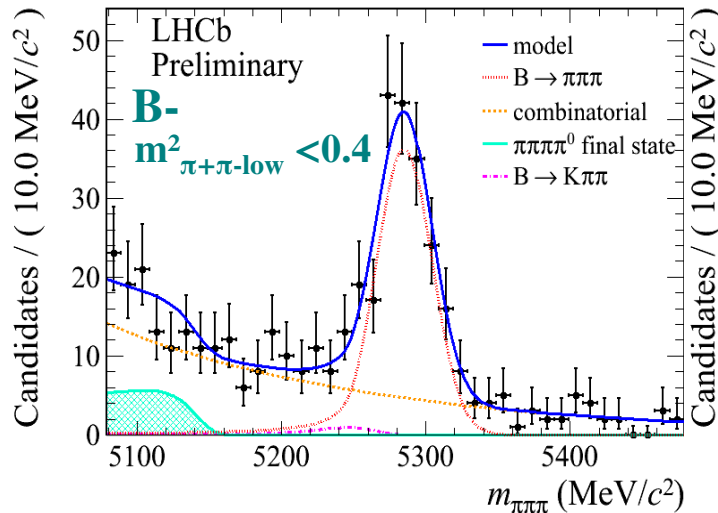
Very large CPV at low $m^2_{\pi^+\pi^- \text{ low}}$ and $m^2_{\pi^+\pi^- \text{ high}} < 15 \text{ GeV}^2/c^4$ not clearly associated to a resonance

$B^\pm \rightarrow \pi^\pm \pi^+ \pi^-$ zoom in large CPV region

Event yield for $m^2_{\pi^+\pi^- \text{high}} > 15$

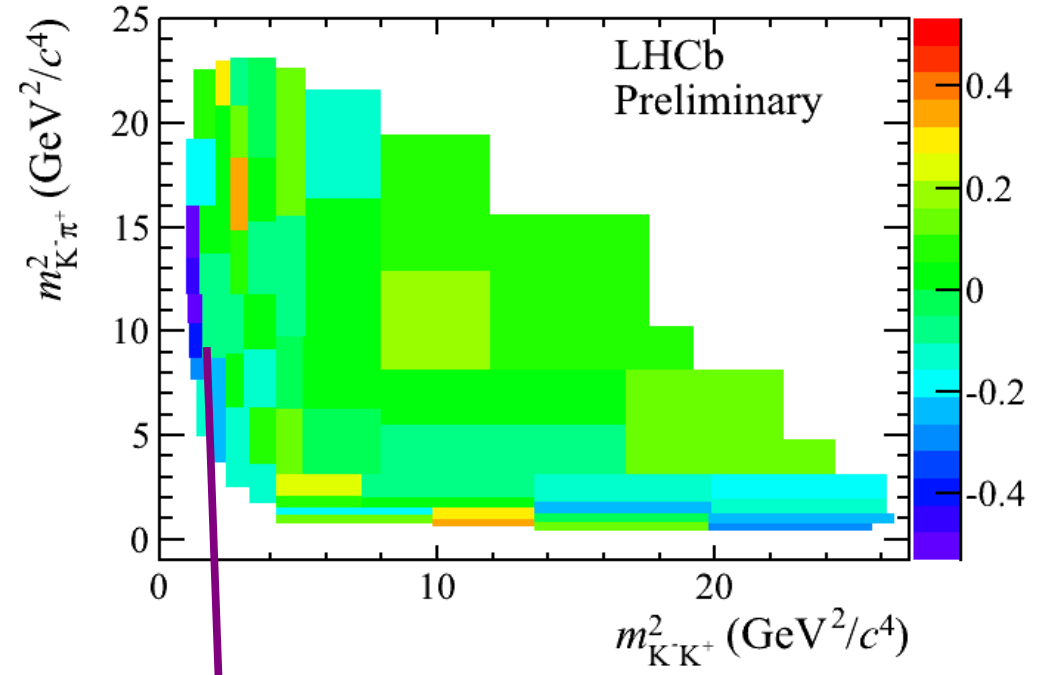
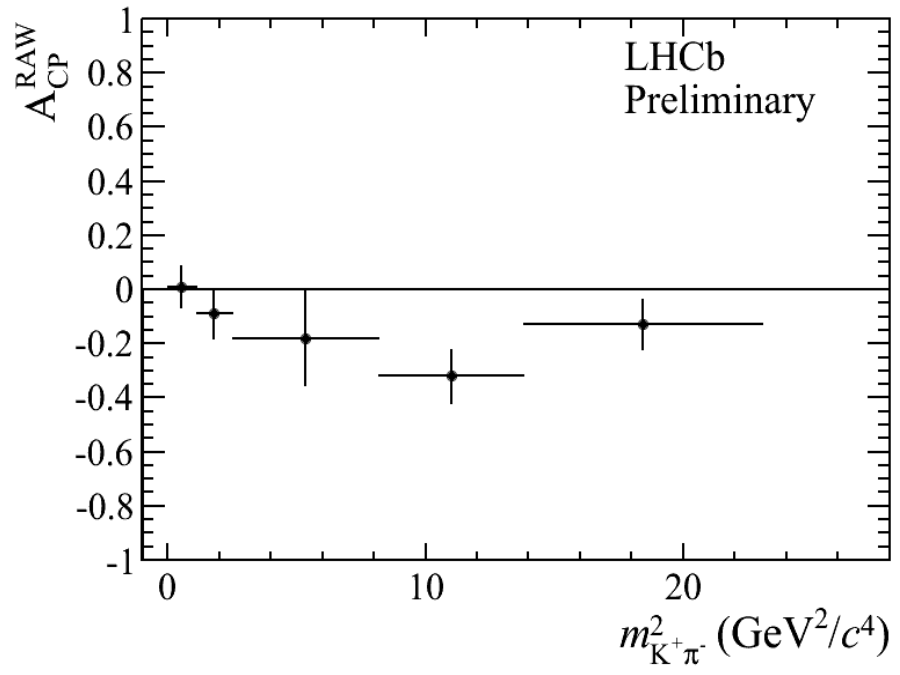


Very large CPV in a region of the phase space not associated to a resonance

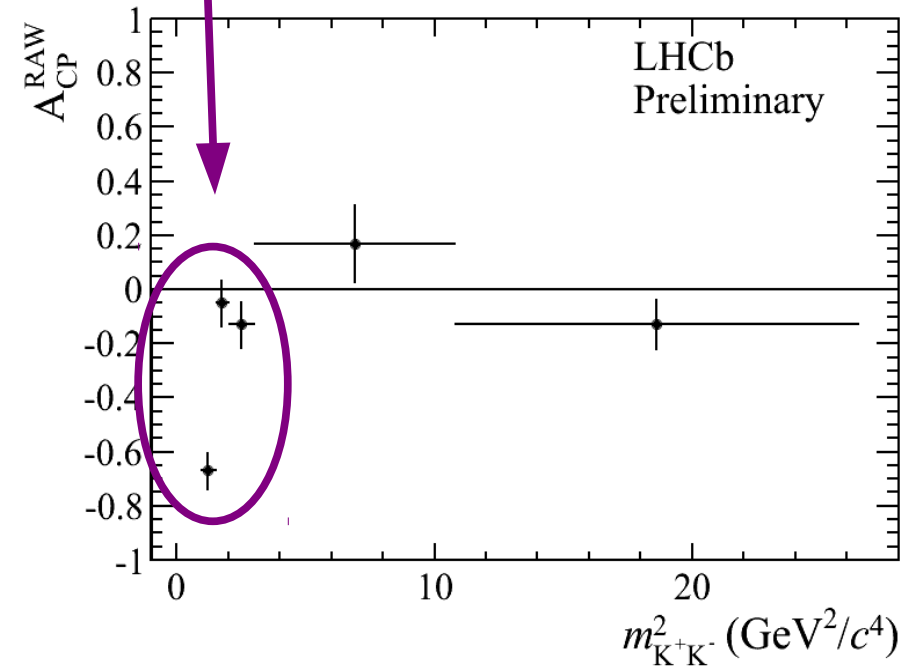


$$A_{cp}(B^\pm \rightarrow \pi\pi\pi \text{ region}) = +0.622 \pm 0.075(\text{stat}) \pm 0.032(\text{syst}) \pm 0.007 (J/\psi K^\pm)$$

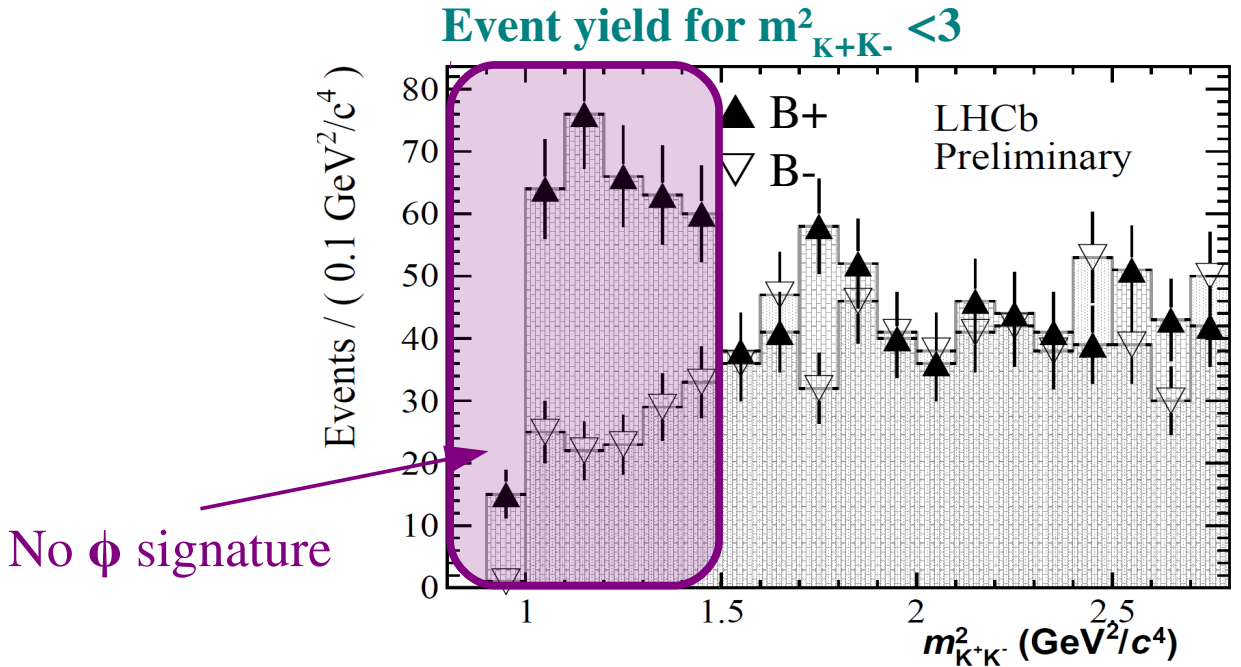
7.6 σ



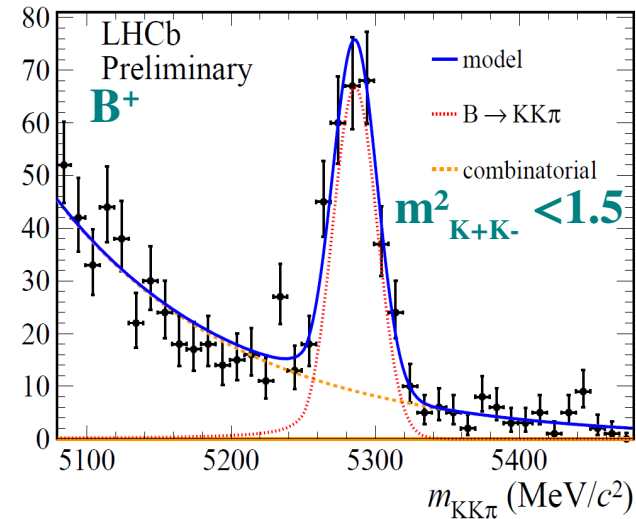
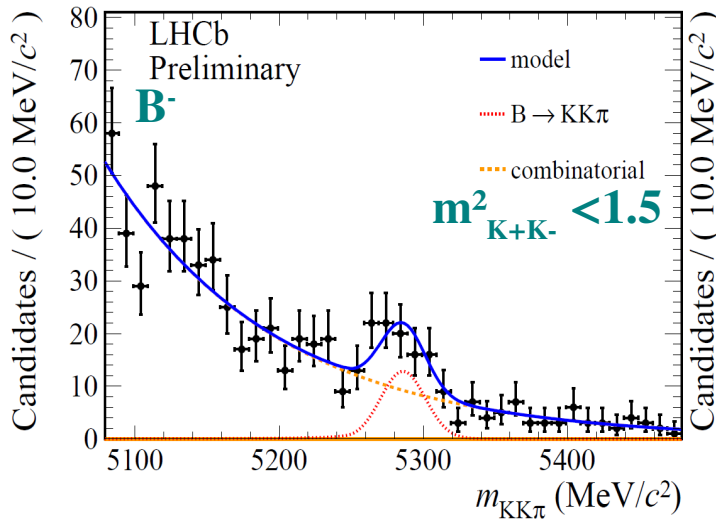
Very large CPV at low $m_{K^+K^-}^2$



$B^\pm \rightarrow \pi^\pm K^+ K^-$ zoom in large CPV region



Very large CPV in a region of the phase space not associated to a resonance



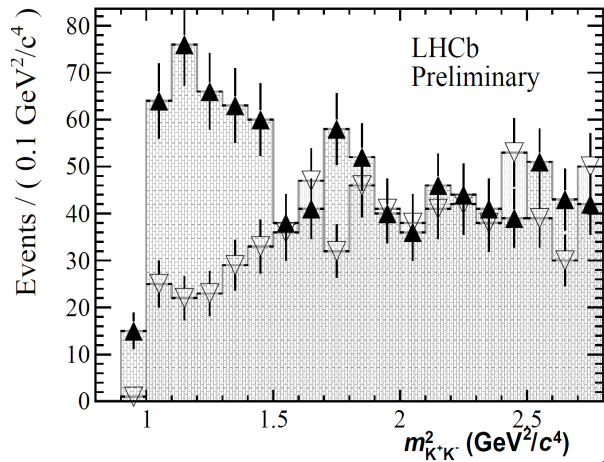
$A_{cp}(B^\pm \rightarrow \pi KK \text{ region}) = -0.671 \pm 0.067(\text{stat}) \pm 0.028(\text{syst}) \pm 0.007 (J/\psi K^\pm)$


9.2 σ




BaBar results on $B^\pm \rightarrow \pi^\pm K^+ K^-$

- BaBar have similar results (but they didn't divide their sample in B^+ and B^-):





$B^+ \rightarrow K^+ K^- \pi^+$



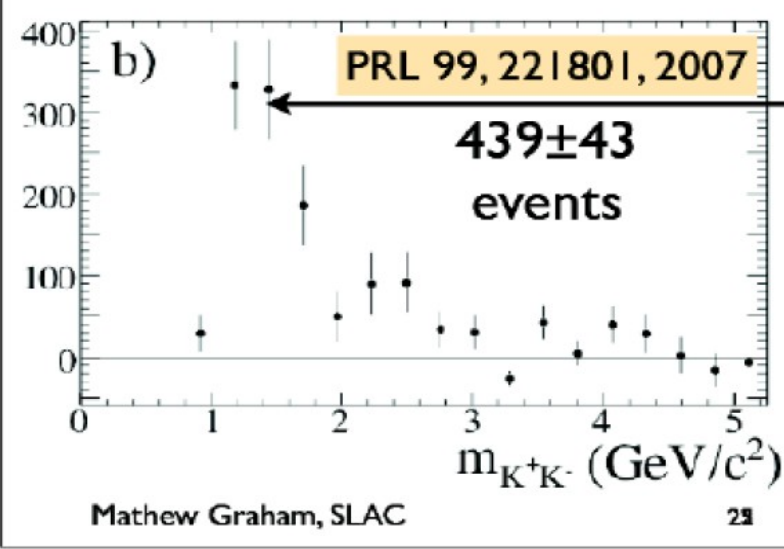
Surprisingly large rate seen in $B^+ \rightarrow K^+ K^- \pi^+$; no evidence for $\phi \pi^+$

$\mathcal{B}(B^+ \rightarrow K^+ K^- \pi^+) = (5.0 \pm 0.5 \pm 0.5) \times 10^{-6}$

~ 1/2 of the events seen at low $K^+ K^-$ mass; structure at ~1.5 GeV?
Similar broad structures seen in $K^+ K^- K^+ / K^+ K^- K_S$ and $\pi^+ \pi^- K^+ / \pi^+ \pi^- K_S$

What about $K_S K_S \pi^+$?

Matt Graham
SLAC
on behalf of the BaBar Collaboration
February 12, 2009
Aspen Winter Conference



~ 1/2 of the events seen at low $K^+ K^-$ mass; structure at ~1.5 GeV?
Similar broad structures seen in $K^+ K^- K^+ / K^+ K^- K_S$ and $\pi^+ \pi^- K^+ / \pi^+ \pi^- K_S$

What about $K_S K_S \pi^+$?

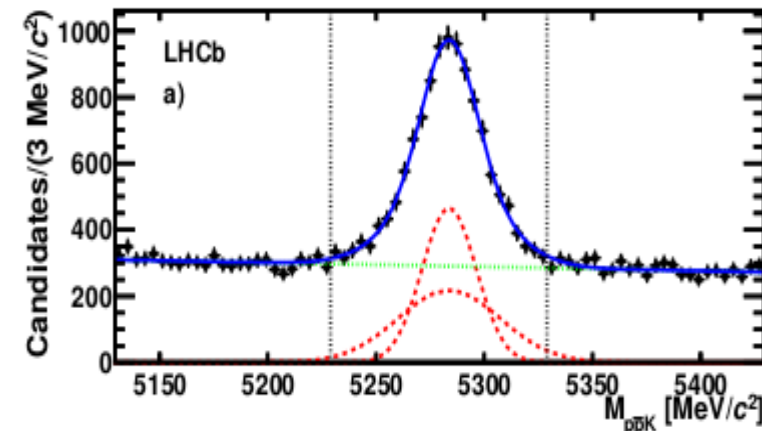
Matt Graham
SLAC
on behalf of the BaBar Collaboration
February 12, 2009
Aspen Winter Conference

Measurements of the BR of $B^+ \rightarrow p\bar{p}K^+$ decays

LHCb-PAPER-2012-047

- Selection explores the decay topology:
 - Tracks with high momentum and transverse momentum.
 - Tracks with large impact parameters with respect to the interaction point.
 - B candidate with large flight distance, momentum and small impact parameter with respect to interaction point.
- A (BDT) selection is trained after the first selection:
 - Simulation used as signal sample.
 - Data from sidebands used as background events.
- Particle ID used to separate protons from kaons and pions.
- Paper reports the measurement of the ration of branching fractions:

B^\pm : 6951 ± 176

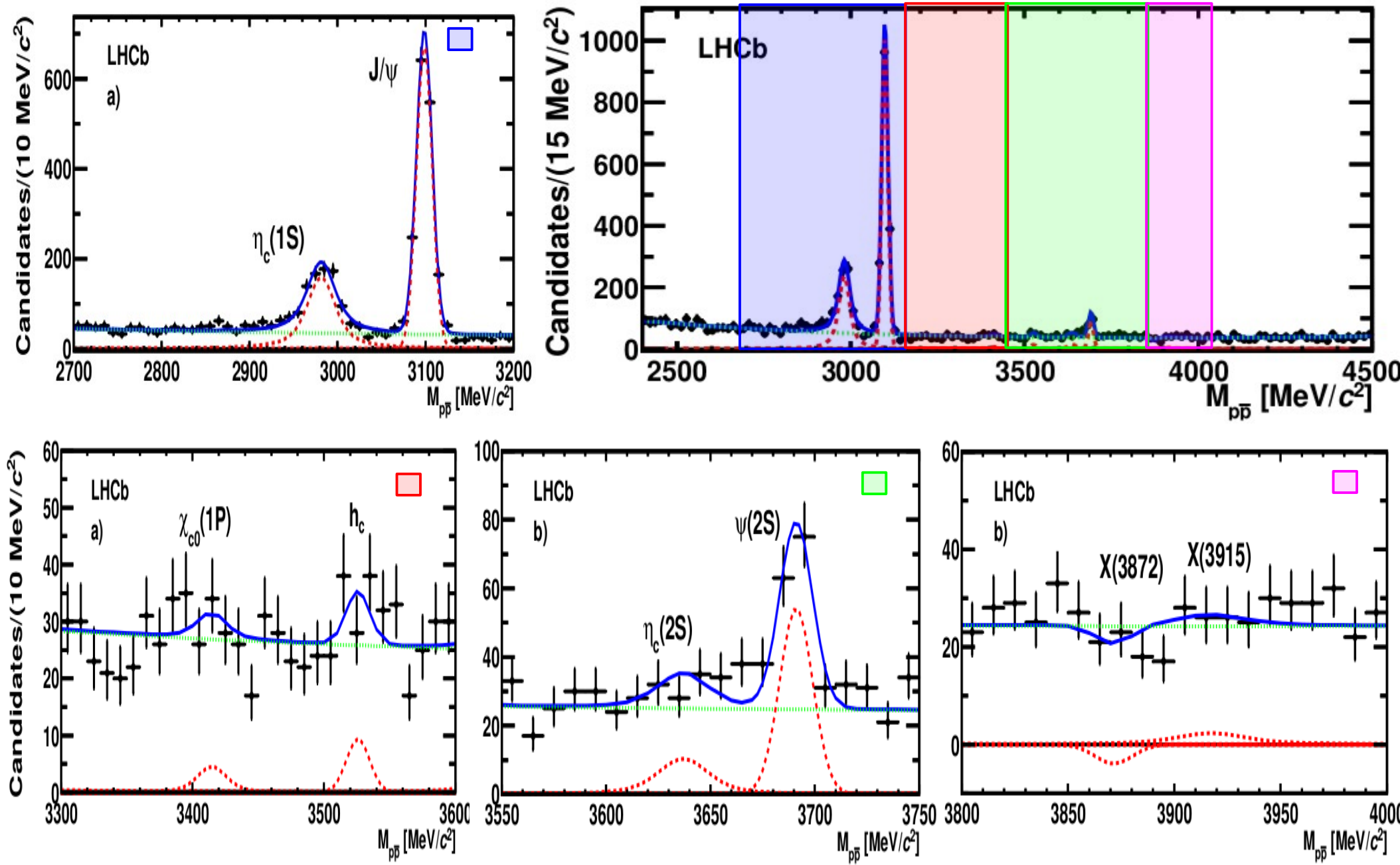


$$\mathcal{R}(\text{mode}) = \frac{\mathcal{B}(B^+ \rightarrow \text{mode} \rightarrow p\bar{p}K^+)}{\mathcal{B}(B^+ \rightarrow J/\psi K^+ \rightarrow p\bar{p}K^+)} = \frac{N_{\text{mode}}}{N_{J/\psi}} \times \frac{\epsilon_{J/\psi}}{\epsilon_{\text{mode}}}$$

- “Mode” holds for intermediate states together with a kaon and ϵ is the total selection efficiency.



$B^+ \rightarrow p\bar{p}K^+$ intermediate states



- Yields summary:

B^+ decay mode	Signal yield	Upper limit (95% CL)
$p\bar{p}K^+$ [total]	6951 ± 176	
$p\bar{p}K^+$ [$M_{p\bar{p}} < 2.85 \text{ GeV}/c^2$]	3238 ± 122	
$J/\psi K^+$	1458 ± 42	
$\eta_c(1S)K^+$	856 ± 46	
$\psi(2S)K^+$	107 ± 16	
$\eta_c(2S)K^+$	39 ± 15	< 65.4
$\chi_{c0}(1P)K^+$	15 ± 13	< 38.1
$h_c(1P)K^+$	21 ± 11	< 40.2
$X(3872)K^+$	-9 ± 8	< 10.3
$X(3915)K^+$	13 ± 17	< 42.1

- Relatives branching fractions and upper limits for $\eta_c(2S)$ and $X(3872)$:

$$\frac{\mathcal{B}(B^+ \rightarrow p\bar{p}K^+)_{\text{total}}}{\mathcal{B}(B^+ \rightarrow J/\psi K^+ \rightarrow p\bar{p}K^+)} = 4.91 \pm 0.19 \text{ (stat)} \pm 0.14 \text{ (syst)},$$

$$\frac{\mathcal{B}(B^+ \rightarrow p\bar{p}K^+)_{M_{p\bar{p}} < 2.85 \text{ GeV}/c^2}}{\mathcal{B}(B^+ \rightarrow J/\psi K^+ \rightarrow p\bar{p}K^+)} = 2.02 \pm 0.10 \text{ (stat)} \pm 0.08 \text{ (syst)},$$

$$\frac{\mathcal{B}(B^+ \rightarrow \eta_c(1S)K^+ \rightarrow p\bar{p}K^+)}{\mathcal{B}(B^+ \rightarrow J/\psi K^+ \rightarrow p\bar{p}K^+)} = 0.578 \pm 0.035 \text{ (stat)} \pm 0.025 \text{ (syst)},$$

$$\frac{\mathcal{B}(B^+ \rightarrow \psi(2S)K^+ \rightarrow p\bar{p}K^+)}{\mathcal{B}(B^+ \rightarrow J/\psi K^+ \rightarrow p\bar{p}K^+)} = 0.080 \pm 0.012 \text{ (stat)} \pm 0.009 \text{ (syst)}.$$

$$\frac{\mathcal{B}(\eta_c(2S) \rightarrow p\bar{p})}{\mathcal{B}(\eta_c(2S) \rightarrow K\bar{K}\pi)} < 3.1 \times 10^{-2}$$

$$\frac{\mathcal{B}(X(3872) \rightarrow p\bar{p})}{\mathcal{B}(X(3872) \rightarrow J/\psi\pi^+\pi^-)} < 2.0 \times 10^{-3}$$

- Evidence of CPV in $B^\pm \rightarrow K^\pm \pi^+ \pi^-$ and $B^\pm \rightarrow K^\pm K^+ K^-$
[LHCb-CONF-2012-018](#) preliminary $\mathcal{L} = 1.0 \text{ fb}^{-1}$

$$A_{\text{cp}}(B^\pm \rightarrow K\pi\pi) = +0.034 \pm 0.009(\text{stat}) \pm 0.004(\text{syst}) \pm 0.007(\text{J}/\psi K^\pm)$$

2.8 σ

$$A_{\text{cp}}(B^\pm \rightarrow KKK) = -0.046 \pm 0.009(\text{stat}) \pm 0.005(\text{syst}) \pm 0.007(\text{J}/\psi K^\pm)$$

3.7 σ

- Evidence of CPV in $B^\pm \rightarrow \pi^\pm \pi^+ \pi^-$ and $B^\pm \rightarrow \pi^\pm K^+ K^-$
[LHCb-CONF-2012-028](#) preliminary $\mathcal{L} = 1.0 \text{ fb}^{-1}$

$$A_{\text{cp}}(B^\pm \rightarrow \pi\pi\pi) = +0.120 \pm 0.020(\text{stat}) \pm 0.019(\text{syst}) \pm 0.007(\text{J}/\psi K^\pm)$$

4.2 σ

$$A_{\text{cp}}(B^\pm \rightarrow \pi KK) = -0.153 \pm 0.046(\text{stat}) \pm 0.019(\text{syst}) \pm 0.007(\text{J}/\psi K^\pm)$$

3.0 σ

- Observation of very high CPV in regions of the Dalitz plot

$$A_{\text{cp}}(B^\pm \rightarrow \pi\pi\pi \text{ region}) = +0.622 \pm 0.075(\text{stat}) \pm 0.032(\text{syst}) \pm 0.007(\text{J}/\psi K^\pm)$$

7.6 σ

$$A_{\text{cp}}(B^\pm \rightarrow \pi KK \text{ region}) = -0.671 \pm 0.067(\text{stat}) \pm 0.028(\text{syst}) \pm 0.007(\text{J}/\psi K^\pm)$$

9.2 σ

- Measurements of the branching fraction of $B^+ \rightarrow p\bar{p}K^+$ decays.
[LHCb-PAPER-2012-047](#) preliminary $\mathcal{L} = 1.0 \text{ fb}^{-1}$

$$\frac{\mathcal{B}(B^+ \rightarrow p\bar{p}K^+)_{\text{total}}}{\mathcal{B}(B^+ \rightarrow J/\psi K^+ \rightarrow p\bar{p}K^+)} = 4.91 \pm 0.19 \text{ (stat)} \pm 0.14 \text{ (syst)},$$

$$\frac{\mathcal{B}(B^+ \rightarrow p\bar{p}K^+)_{M_{p\bar{p}} < 2.85 \text{ GeV}/c^2}}{\mathcal{B}(B^+ \rightarrow J/\psi K^+ \rightarrow p\bar{p}K^+)} = 2.02 \pm 0.10 \text{ (stat)} \pm 0.08 \text{ (syst)},$$

$$\frac{\mathcal{B}(B^+ \rightarrow \eta_c(1S)K^+ \rightarrow p\bar{p}K^+)}{\mathcal{B}(B^+ \rightarrow J/\psi K^+ \rightarrow p\bar{p}K^+)} = 0.578 \pm 0.035 \text{ (stat)} \pm 0.025 \text{ (syst)},$$

$$\frac{\mathcal{B}(B^+ \rightarrow \psi(2S)K^+ \rightarrow p\bar{p}K^+)}{\mathcal{B}(B^+ \rightarrow J/\psi K^+ \rightarrow p\bar{p}K^+)} = 0.080 \pm 0.012 \text{ (stat)} \pm 0.009 \text{ (syst)}.$$

- The upper limits obtained challenges some predictions for the molecular interpretations of the X(3872):

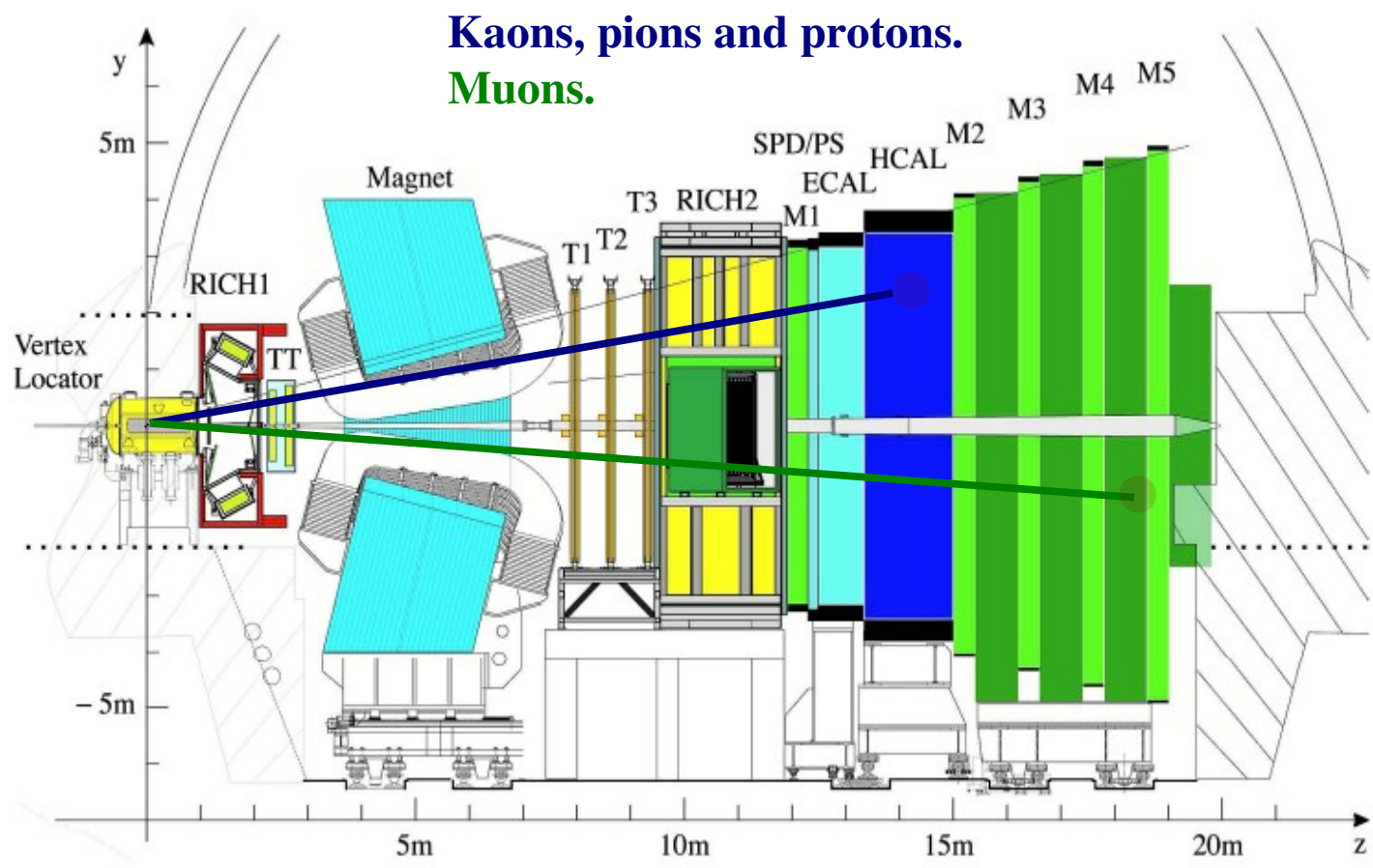
G. Chen, et. al: **PRD 77**, (2008) 097501 and E. Braaten, et. al: **PRD 77**, (2008) 034019

$$\frac{\mathcal{B}(\eta_c(2S) \rightarrow p\bar{p})}{\mathcal{B}(\eta_c(2S) \rightarrow K\bar{K}\pi)} < 3.1 \times 10^{-2}$$

$$\frac{\mathcal{B}(X(3872) \rightarrow p\bar{p})}{\mathcal{B}(X(3872) \rightarrow J/\psi\pi^+\pi^-)} < 2.0 \times 10^{-3}$$

Three times more statistics available.
 New results soon!

Backup



- Excellent tracking and vertexing for B and D decays.
- Excellent particle identification.
- Kaons, pions and protons travels through substantial amount of material.
 - Possible detection asymmetry is accounted for.

Final selection for $B \rightarrow hhh$, $h = K$ or π

- Trigger decision:
 - Hardware trigger (L0) to select a hadron with high transverse energy.
 - Software trigger (Hlt) to select hadrons with high transverse momentum and coming from the same decaying vertex
- PID selection:
 - $\Delta \log \mathcal{L}_{K\pi} > 4$ for kaons and $\Delta \log \mathcal{L}_{K\pi} < 0$ for pions.
 - Muon veto : $\Delta \log \mathcal{L}_{\mu\pi} < 5$ to exclude the control channel (see below).
 - Cuts on invariant masses $m_{\pi\pi}$, $m_{K\pi}$ and m_{KK} to exclude charm background.
- Offline selection explore the decay topology:
 - Tracks momenta and impact parameter with respect to interaction point and decaying vertex.
 - B candidate flight distance, momentum and impact parameter with respect to interaction point.

Variables	Selection cuts
Tracks P_T	$> 0.1 \text{ GeV}/c$
Tracks P	$> 1.5 \text{ GeV}/c$
Tracks IP χ^2	> 1
Tracks $\chi^2/\text{n.d.f.}$	< 3
Sum of P_T of tracks	$> 4.5 \text{ GeV}/c$
Sum of IP χ^2 of tracks	> 200
P_T of the highest- P_T track	$> 1.5 \text{ GeV}/c$
P_T of the second highest- P_T track	$> 0.9 \text{ GeV}/c$
IP of the highest- P_T track	$> 0.05 \text{ mm}$
Maximum DOCA	$< 0.2 \text{ mm}$
B^\pm candidate M_{KKK}	$5.05 - 6.30 \text{ GeV}/c^2$
B^\pm candidate M_{KKK}^{COR}	$4 - 7 \text{ GeV}/c^2$
B^\pm candidate M^{COR}	$< 5.8 \text{ GeV}/c^2$
B^\pm candidate IP χ^2	< 10
B^\pm candidate P_T	$> 1.7 \text{ GeV}/c$
Distance from SV to any PV	$> 3 \text{ mm}$
Secondary Vertex χ^2	< 12
B^\pm candidate $\cos(\theta)$	> 0.99998
B^\pm Pointing angle	< 0.1
B^\pm Flight Distance χ^2	> 700
Number of long tracks in the event	< 200



$B^\pm \rightarrow K^\pm \pi^+ \pi^-$ and $B^\pm \rightarrow K^\pm K^+ K^-$ Fit function

- We performed an unbinned extended likelihood fit to the B^\pm invariant mass
- Signal PDF model:
 - Sum of a Crystal Ball and a Gaussian
 - Common mean and different widths for the two functions.
 - Fractions and Crystal Ball parameters extracted from MC and fixed to data.
 - Widths for both Crystal Ball and Gaussian determined from the fit to full data.
- Combinatorial background PDF model:
 - Exponential function with one free parameter for the slope.
- Peaking and partial backgrounds PDF model:
 - Modified Gaussian with shapes extracted from MC and fixed to data for peaking and partial backgrounds.
 - Fractions extracted from MC for peaking background and left float in the fit for partial background.

Signal PDF: Gaussian + Crystal Ball.

$$F_S(m) = f_{\text{sig}} \mathcal{G}(m; m_0, \sigma_1) + (1 - f_{\text{sig}}) \mathcal{C}(m; m_0, \sigma_2, a, n)$$

Background PDF: Modified Gaussian.

$$F_i(m) = N_i \exp \left[\frac{-(m - \mu_i)^2 \beta_i(m)}{2\sigma_{Ri}^2} \right], \quad \beta_i(m) = \exp(-2\lambda_i(m - \mu_i))$$



$B^\pm \rightarrow K^\pm \pi^+ \pi^-$ and $B^\pm \rightarrow K^\pm K^+ K^-$ systematics and results

- Signal PDF: floated parameters in the fit procedure and two Crystal Balls used.
- Signal shape: signal yield from the difference between the total number of events and the background integral inside signal region.
- Background model: background fraction varied for both $K\pi\pi$ and KKK modes.
- Background charge asymmetry: fit with 100% charge asymmetry for the peaking background components.
- Acceptance: raw asymmetry corrected by the efficiency in each bin of the phase space.
- Subtraction method: kinematic variables of the kaon from control channel were weighted to match the same distribution from the signal kaon.

Contribution	Syst($K^\pm \pi^+ \pi^-$)	Syst($K^\pm K^+ K^-$)
Signal fixed parameters	0.002	0.002
Signal model	0.0001	0.0001
Signal shape	0.0012	0.0001
Background model	0.0003	0.00002
Background asymmetry	0.0002	0.0001
Acceptance	0.001	0.0015
Trigger correction	0.0011	0.001
Subtraction method	0.0035	0.0012
Total	0.0045	0.0030

$$A_{cp}(B^\pm \rightarrow K\pi\pi) = +0.034 \pm 0.009(\text{stat}) \pm 0.004(\text{syst}) \pm 0.007^*$$

$$A_{cp}(B^\pm \rightarrow KKK) = -0.046 \pm 0.009(\text{stat}) \pm 0.005(\text{syst}) \pm 0.007^*$$

* $J/\psi K$ A_{cp} uncertainty quoted separately.

$$A_{cp}(B^\pm \rightarrow K\pi\pi) = +0.038 \pm 0.022$$

$$A_{cp}(B^\pm \rightarrow KKK) = -0.017 \pm 0.030$$



$$B^{\pm} \rightarrow \pi^{\pm}\pi^{+}\pi^{-} \text{ and } B^{\pm} \rightarrow \pi^{\pm}K^{+}K^{-}$$

Fit function

- We performed an unbinned extended likelihood fit to the B^{\pm} invariant mass.
- Signal PDF model:
 - Crystal Ball function.
 - Crystal Ball radiative tail parameters extracted from MC and fixed to data.
 - Crystal Ball mean and width extracted from the combined B^{+}/B^{-} data and fixed to the individual B^{+} and B^{-} fits.
- Combinatorial background PDF model:
 - Exponential function with one free parameter for the slope for $B^{\pm} \rightarrow \pi^{\pm}\pi^{+}\pi^{-}$.
 - A modified Gaussian for $B^{\pm} \rightarrow \pi^{\pm}K^{+}K^{-}$.
- Peaking and partial backgrounds PDF model:
 - Modified Gaussian with shapes extracted from MC and fixed to data for peaking and partial backgrounds for $B^{\pm} \rightarrow \pi^{\pm}\pi^{+}\pi^{-}$.
 - Negligible for $B^{\pm} \rightarrow \pi^{\pm}K^{+}K^{-}$.

$B^\pm \rightarrow \pi^\pm \pi^+ \pi^-$ and $B^\pm \rightarrow \pi^\pm K^+ K^-$ systematics and results

- Fit function: signal yield from the difference between the total number of events and the background integral inside signal region.
- Acceptance efficiency: error of the efficiency correction R.
- Kaon kinematics: the $B^\pm \rightarrow J/\psi K^\pm$ raw asymmetry in bins of kaon momentum is weighted by the ratio of K^- and K^+ efficiencies from $D^0 \rightarrow K^+ K^-$ sample.
- Kaon instrumental asymmetry: the statistical uncertainty of the kaon instrumental asymmetry was included as a systematic since it came from another analysis.
- Pion instrumental asymmetry: the statistical uncertainty of the pion instrumental asymmetry was included as a systematic since it came from another analysis.

Contribution	$\pi\pi\pi$	$KK\pi$
Fit function model	0.008	0.009
Acceptance	0.015	0.014
A_D^K kaon kinematics	0.008	0.008
A_D^K stat. uncertainty	0.002	0.002
A_D^π stat. uncertainty	0.003	0.003
Total	0.019	0.019

$$A_{cp}(B^\pm \rightarrow \pi\pi\pi) = +0.120 \pm 0.020(\text{stat}) \pm 0.019(\text{syst}) \pm 0.007^*$$

$$A_{cp}(B^\pm \rightarrow \pi KK) = -0.153 \pm 0.046(\text{stat}) \pm 0.019(\text{syst}) \pm 0.007^*$$

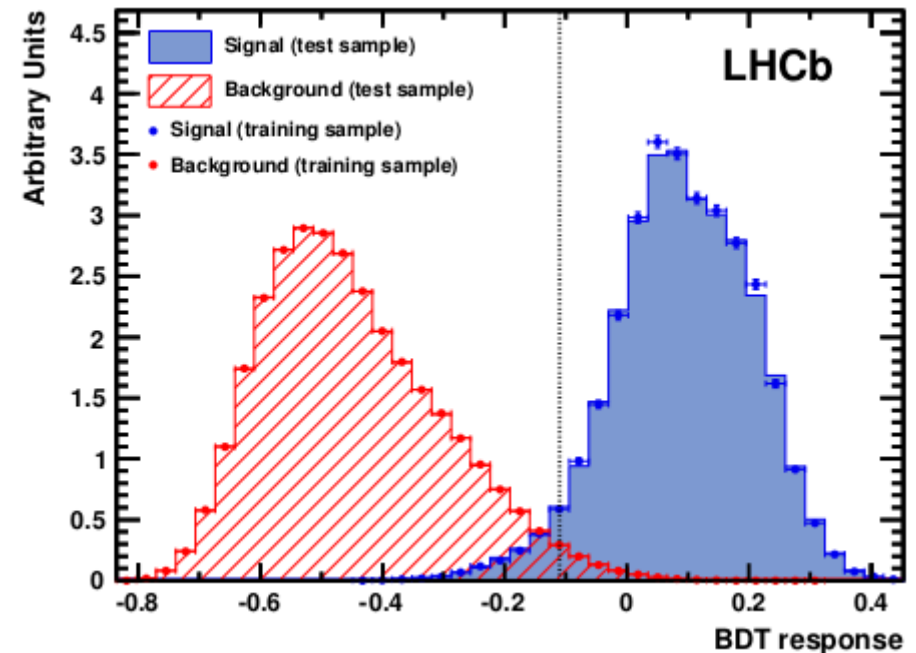
* $J/\psi K$ A_{cp} uncertainty quoted separately.

$$A_{cp}(B^\pm \rightarrow \pi\pi\pi) = +0.032 \pm 0.044(\text{stat}) \begin{matrix} +0.040 \\ -0.037 \end{matrix}(\text{syst})$$

$$A_{cp}(B^\pm \rightarrow \pi KK) = -0.00 \pm 0.10(\text{stat}) \pm 0.03(\text{syst})$$

BDT variables for $B^+ \rightarrow p\bar{p}K^+$ decays

- The p_T of each track;
- Sum of the daughters' p_T ;
- Sum of the $IP\chi^2$ of the three daughter tracks with respect to the primary vertex;
- IP of the daughter with the highest p_T with respect to the primary vertex;
- The number of daughters with $p_T > 900$ MeV/c;
- Maximum distance of closest approach between any two daughters;
- IP of the B candidate with respect to any primary vertex;
- Distance between the primary and secondary vertices;
- The angle between the flight direction and the z axis of the detector;
- The pointing variable defined as: $\frac{P \sin \theta}{P \sin \theta + \sum_i p_{T,i}}$
- The log likelihood difference for each daughter between the assumed PID hypothesis and the pion hypothesis.



- The BDT response is chosen in order to have a signal over background ratio of the order of unity and this corresponds to a response value of -0.11.
- The BDT response efficiency is greater than 92% with a background rejection of 86%.

Table 2: Relative systematic uncertainties (in %) on the relative branching fractions from different sources. The total systematic uncertainty is determined by adding the individual contributions in quadrature.

Source	$\mathcal{R}(\text{total})$	$\mathcal{R}(M_{p\bar{p}} < 2.85 \text{ GeV}/c^2)$	$\mathcal{R}(\eta_c(1S))$	$\mathcal{R}(\psi(2S))$
Efficiency ratio	0.21	0.5	3.3	4.8
B^+ mass fit range	0.16	0.5	–	–
Sig. and Bkg. shape	2.5	3.6	1.8	6.5
B^+ mass window	0.6	0.6	0.9	3.8
Non-signal component	–	–	0.4	5.1
Signal tail param.	1.0	1.0	1.2	4.3
Total	2.8	3.8	4.1	11.3

Source	$\mathcal{R}(\eta_c(2S))$	$\mathcal{R}(\chi_{c0}(1P))$	$\mathcal{R}(h_c(1P))$	$\mathcal{R}(X(3872))$	$\mathcal{R}(X(3915))$
Efficiency ratio	4.4	2.5	3.4	6.5	7.0
B^+ mass fit range	–	–	–	–	–
Sig. and Bkg. shape	3.9	3.3	14.3	5.6	10.1
B^+ mass window	11.3	23.6	23.6	17.5	7.5
Non-signal component	–	–	–	–	–
Signal tail param.	1.0	1.0	1.0	1.0	1.0
Total	12.8	24.0	27.8	19.5	15.5